SECURITY

AD-A216 697

THE FILE COPY

(2)

REPORT DOCUMENTATION PAGE

DTIC ELECTE JAN 12 1990 S D

1a. REPORT SECURITY CLASSIFICATION: Unclassified	1b. RESTRICTIVE MARKINGS
2a. SECURITY CLASSIFICATION AUTHORITY	3. DISTRIBUTION/AVAILABILITY OF REPORT: Approved for public release, distribution unlimited
2b. DECLASSIFICATION/DOWNGRADING SCHEDULE	
4. PERFORMING ORGANIZATION REPORT NUMBER(S): AFOSR 86-0158	5. MONITORING ORGANIZATION REPORT NUMBER(S): AFOSR.TR. 89-1688
6a. NAME OF PERFORMING ORGANIZATION: Stanford University; 6b. OFFICE SYMBOL (If applicable)	7a. NAME OF MONITORING ORGANIZATION: AFOSR
6c. ADDRESS (City, State, and ZIP Code): Dept. Mat. Sci. & Engr., Stanford University, Stanford, CA 94305-2205	7b. ADDRESS (City, State, and ZIP Code): BLDG 410, BAFB DC 20332-6448
8a. NAME OF FUNDING/SPONSORING ORGANIZATION: AFOSR; 8b. OFFICE SYMBOL (If applicable)	9. PROCUREMENT INSTRUMENT IDENTIFICATION NUMBER: AFOSR 86-0158
8c. ADDRESS (City, State, and ZIP Code): Department of the Air Force, Building 410, Bolling Air Force Base, DC 20332-6448	10. SOURCE OF FUNDING NUMBERS: PROGRAM ELEMENT NO. 61102F; PROJECT NO. 2306; TASK NO. B1; WORK UNIT ACCESSION NO.

11. TITLE (Include Security Classification)

Crystal Growth and Mechanical Properties of Semiconductor Alloys

12. PERSONAL AUTHOR(S)

Professor David A. Stevenson

13a. TYPE OF REPORT	13b. TIME COVERED	14. DATE OF REPORT (Year, Month, Day)	15. PAGE COUNT
Final Report	FROM 4/15/86 TO 4/15/89	November 1, 1989	44

16. SUPPLEMENTARY NOTATION

17. COSATI CODES			18. SUBJECT TERMS (Continue on reverse if necessary and identify by block number)
FIELD	GROUP	SUB-GROUP	

19. ABSTRACT (Continue on reverse if necessary and identify by block number)

We describe a study of the mechanical properties and crystal growth of compound semiconductor alloys. There are significant results in five major areas: (1) hardness measurements of $Hg_{1-x}Cd_xTe$ of different compositions of layers grown on CdTe substrates; (2) the growth and the measurement of hardness and interdiffusion of $Hg_{1-x}Zn_xTe$ of different compositions on ZnTe substrates; (3) the measurements of hardness and elastic modulus of thin film and bulk samples of CdTe, of thin film and bulk samples of ZnTe, and of unannealed and annealed ZnTe-CdTe superlattices; and (5) the growth and hardness measurement of bulk samples of $Ga_xIn_{1-x}Sb$. We also investigated experimental conditions that may influence the hardness values and, hence, might explain the large variations in hardness values that are described in the literature for many semiconductors, specifically the following: (1) differences in the hardness of different grains, across twins, and as the sample is rotated that may arise from crystal orientation effects; (2) differences in hardness arising from the photoplastic effect; and (3) differences in hardness arising from differences in applied loads during hardness testing

20. DISTRIBUTION/AVAILABILITY OF ABSTRACT	21. ABSTRACT SECURITY CLASSIFICATION
☒ UNCLASSIFIED/UNLIMITED ☐ SAME AS RPT ☐ DTIC USERS	Unclassified
22a. NAME OF RESPONSIBLE INDIVIDUAL: MAJOR GERNOT POMRENKE	22b. TELEPHONE (Include Area Code): (202) 767-4931; 22c. OFFICE SYMBOL: NE

DD FORM 1473, 84 MAR — 83 APR edition may be used until exhausted. All other editions are obsolete. SECURITY CLASSIFICATION OF THIS PAGE

☆ U.S. Government Printing Office: 1986—607-044

Air Force Office of Scientific Research

Final Report AFOSR-TR- 89-1588

November 1989

Contract AFOSR 86-0158
Project Task 2306/B1

"Crystal Growth and Mechanical Properties of Semiconductor Alloys"

Principal Investigator: D. A. Stevenson

Department of Materials Science and Engineering
Stanford University
Stanford, CA 94305

Sponsored by
Air Force Office of Scientific Research

ABSTRACT

We describe a study of the mechanical properties and crystal growth of compound semiconductor alloys. There are significant results in five major areas: (1) hardness measurements of $Hg_{1-x}Cd_xTe$ of different compositions of layers grown on CdTe substrates; (2) the growth and the measurement of hardness and interdiffusion of $Hg_{1-x}Zn_xTe$ of different compositions on ZnTe substrates; (3) the measurement of hardness and elastic modulus of HgCdTe and HgZnTe epilayers on ZnCdTe substrates; (4) the measurement of hardness and elastic modulus of thin film and bulk samples of CdTe, of thin film and bulk samples of ZnTe, and of unannealed and annealed ZnTe-CdTe superlattices; and (5) the growth and hardness measurement of bulk samples of $Ga_xIn_{1-x}Sb$. We also investigated experimental conditions that may influence the hardness values and, hence, might explain the large variations in hardness values that are described in the literature for many semiconductors, specifically the following: (1) differences in the hardness of different grains, across twins, and as the sample is rotated that may arise from crystal orientation effects; (2) differences in hardness arising from the photoplastic effect; and (3) differences in hardness arising from differences in applied loads during hardness testing.

We propose to continue this work by: (1) expanding our study on a wider range of composition of ZnTe-CdTe superlattices; (2) investigating both strained layer and lattice matched superlattices of InGaAsP; (3) investigating superlattices of Si and Ge; and (4) investigating creep in HgTe and other semiconductors of relatively low melting temperatures. Hardness and elastic modulus will be measured using a Nanoindenter. X-ray diffraction and cross section TEM of both unannealed and annealed superlattices will be used to characterize the samples and examine the strain and dislocation structure. Time and resources permitting, we will also use two growth techniques: (1) the ISOVPE method to grow ternary semiconductors; and (2) the vertical Bridgman method to grow coarse grained ingots of selected ternary semiconductors.

I. Introduction

The mechanical properties of semiconductor materials is a topic of practical and theoretical interest. The mechanical properties relate to changes in electronic and optical properties that arise during processing of semiconductor devices, particularly from dislocations that are introduced during thermal processing, slicing, polishing, ion implantation, and the application of films. The mechanical strength is also important in the handling of wafers during processing and in the integrity of devices during service. Recent theoretical studies have related hardness in ternary semiconductor alloys to fundamental atomic properties [1], but there is limited opportunity to compare theory to experiment because of a paucity of experimental information.

A major problem is the preparation of bulk samples of semiconductor alloys for conventional mechanical tests. This difficulty arises from a large separation between the liquidus and solidus lines on the pseudobinary phase diagrams for such systems. This phase behavior causes segregation during melt growth and a tendency for interface breakdown, arising from constitutional supercooling [2-6]. As a consequence, most semiconductor alloys are grown as thin films for specific device applications.

The objective of this research program is to explore methods for determining the mechanical properties of semiconductor alloy systems. To achieve this objective, we have explored three approaches: hardness measurements on thick films (10-200 μm) using conventional microhardness techniques; hardness measurements on thin films (< 2 μm) using a Nanoindenter; and hardness measurements on bulk samples that we have prepared. In this study, we have prepared many of our own samples, but we have also aquired several samples from various outside sources. Details of the work are provided below.

II. The Nanoindenter

Most films prepared by MBE or MOCVD are less than one micron thick and conventional microhardness measurements cannot be made on such thin films. Meaningful hardness measurements can be made on such films using a new instrument, the Nanoindenter. The Nanoindenter has several advantages: it is computer controlled; hardness can be obtained over a small area and on very thin films; indentation imaging is not needed; the indentation rate can be varied; and hardness can be monitored continuously with depth. The capabilities and specifications of the Nanoindenter include a minimum indentation depth of 200 Å; a force resolution of 0.5 μN; a displacement resolution of 2-3 Å; and a typical indentation rate of 30 Å/second [7]. Figure 1 shows a typical indentation curve, showing indentation depth as a function of applied load. Since the Nanoindenter

measures and records depth versus load, elastic modulus values can be calculated from the linear portion of the unloading curve. Since the load can be held constant for a programmed time, tests analogous to uniaxial tensile creep tests can be run. The Nanoindenter has emerged as an effective tool for investigating thin films and superlattices.

III. Progress

We have made significant progress in five major areas. These important accomplishments and other work are discussed below.

A. HgCdTe epilayers grown by ISOVPE

A major area of progress is in the growth of and hardness measurements on HgCdTe epitaxial layers. Thick films (5-100 μm) are grown on a substrate using an isothermal vapor phase epitaxial (ISOVPE) method pioneered by Marfaing et al. [8]. An important new refinement of this method was made by Fleming [9], which was further developed in the present study to grow single crystal films of variable composition. There are two important advantages to this variation of the ISOVPE method: it is a relatively simple experimental technique and it produces an oriented single epilayer with a variation in composition. Thick films (~10-100 μm) of HgCdTe were grown on CdTe substrates. The method consists of placing a CdTe substrate in a vertical orientation with respect to a Te-rich HgTe source in an enclosed evacuated quartz ampule and annealing at a constant temperature. Figure 2 is a schematic diagram of the capsule. The resulting epilayer is quite thick (10-100 μm) and conventional microhardness measurements can be made. Furthermore, the composition varies in the epilayer and hardness can be determined as a function of composition for an oriented single crystal layer. Figure 3 shows hardness values as a function of the values of x in the $Hg_{1-x}Cd_xTe$ epilayers ranging from 0.1 to 0.7. The hardness values range from 33 kg/mm^2 (0.33 GPa) to 69 kg/mm^2 (0.69 GPa), which are comparable to hardness values determined by Cole et al. [10] and Triboulet et al. [11]. (Microhardness measurements are typically reported not in S.I. units, but in terms of "kg/mm^2." The conversion factor is: 100 kg/mm^2 is equal to 1 GPa.) Our samples are thick films whereas Triboulet et al. and Cole et al. used bulk HgCdTe samples grown by the travelling heater method and the Bridgman method, respectively. Figure 4 shows how our data compare with the data of Cole et al. [10], Kurilo et al. [12], Sharma et al. [13], Koman and Pashovskii [14], Triboulet et al. [11], and Barbot et al. [15]. Although there is some scatter in our data at higher x values, there is good agreement with the data of Cole et al. and Triboulet et al. Our method is an efficient way to survey a broad range of

composition of a single oriented epilayer rather than measuring separately prepared samples of different composition and orientation.

There is positive deviation of the hardness values from a simple linear variation with composition in HgCdTe. (This deviation is called "bowing.") This enhancement in the hardness of HgCdTe is unexpected, since there is no significant difference in the bond lengths of CdTe and HgTe. Cole et al. [10] describe possible mechanisms for solid solution hardening in HgCdTe. Solid solution hardening may arise from elastic and electrical interactions of solute atoms with dislocations. Fleisher (as cited in Cole et al. [10]) divides the elastic interactions into two misfit parameters: one parameter relates the local strain field arising from the size difference between the solute and matrix atoms; and a second parameter represents a change in the local elastic modulus due to the presence of the solute atom. Cole et al. [10] propose that there may be a change in the local charge relative to the matrix by the addition of Cd or Hg atoms which causes electrical interactions with charged dislocations. Thus, if free carriers produce a screening effect, then, since the free carrier concentration decreases with increasing x from a maximum at $x = 0.1$, the elastic interaction would be the dominant factor contributing to hardening at low x values, while both elastic and electrical interactions contribute at high x values. The hardness would therefore reach a maximum at high values of x, a trend clearly established by the data. Sher et al. [16] have proposed a possible mechanism for solid solution hardening in ternary semiconductor alloys based on fundamental atomic properties. Although pure CdTe and pure HgTe have nearly the same bond lengths (2.81 and 2.80 Å, respectively), their calculations predict that during alloying the HgTe bond length gets smaller and CdTe bond length gets larger. This then causes internal strains on an atomic scale and predicts a slight increase in hardness, but much smaller than observed.

B. HgZnTe epilayers grown by ISOVPE

Our second area of activity is the growth, hardness, and interdiffusion studies of HgZnTe epitaxial layers. HgZnTe is a candidate for infrared detectors since it is predicted to be more stable than HgCdTe. Theoretical work done by A. Sher et al. [16] relates the lattice stability to bond strength and the hardness, in turn, to the bond strength. Thick films (60-100 μm) of HgZnTe are grown on large grained polycrystalline ZnTe substrates by the ISOVPE method using a HgTe source. The samples were cross sectioned, mounted, and polished, and then examined by electron microprobe analysis. Figure 5 shows a typical plot of the composition of a HgZnTe epilayer grown at 550° C for 48 hours as a function of the distance from the surface of the epilayer. This composition profile is very similar to those of epilayers grown by Pobla et al. [17]. Hardness measurements were then made

across the epilayer thickness using a Knoop indenter. Figure 6 shows hardness values as a function of the values of x in the $Hg_{1-x}Zn_xTe$ epilayers. The hardness values range from 30 kg/mm^2 (0.30 GPa) to 175 kg/mm^2 (1.75 GPa) and show good agreement with hardness values of Triboulet et al. [11] and Schenk and Fissel [18]. Our samples are thick films whereas Triboulet et al. and Schenk and Fissel used bulk HgZnTe samples grown by the travelling heater method. Also, we used a Knoop indenter whereas both Triblouet et al. and Schenk and Fissel used a Vickers indenter to measure hardness. So, despite the differences in types of samples and indenters used to measure hardness, our data show excellent agreement with published hardness values for HgZnTe. Bowing in the hardness values as a function of composition arising from hardening enhancement by alloying is also seen in HgZnTe. The hardening enhancement in HgZnTe is due to solid solution hardening arising from the strains induced by the significant difference in the bond lengths of HgTe and ZnTe (5.5%). The bowing in HgZnTe is significantly greater (approximately two times at the highest values) than the bowing seen in HgCdTe.

Interdiffusion coefficients were evaluated from the ISOVPE growth kinetics using a simple geometric analysis of the composition profile obtained in the interdiffusion limited regime. Fleming and Stevenson [19] developed this analysis while studying ISOVPE growth kinetics in HgCdTe. We used the analysis for HgZnTe since the growth kinetics are similar. Our interdiffusion coefficients compare reasonably well (within a factor of two) to data reported by S. Fang et al. [20] and Pobla et al. [17], both of whom used the Boltzmann-Matano method to analyze results from HgTe/ZnTe diffusion couples. Figure 7 shows our results along with those of S. Fang et al. and Pobla et al.

C. HgCdTe and HgZnTe epilayers

A third area of activity is the measurement of the hardness and elastic moduli of HgCdTe and HgZnTe epilayers grown on ZnCdTe substrates by horizontal liquid phase epitaxy (HLPE) and provided by Dr. Mitra Sen of the Santa Barbara Research Center. Two sets of HgCdTe and HgZnTe epilayer samples were studied using the Nanoindenter: (1) an 11.0 μm $Hg_{0.67}Cd_{0.33}Te$ epilayer on a $Cd_{0.96}Zn_{0.04}Te$ substrate (MCT1) and a 26.0 μm $Hg_{0.8}Cd_{0.2}Te$ epilayer on a $Cd_{0.96}Zn_{0.04}Te$ substrate (MCT2); and (2) a 7.7 μm $Hg_{0.76}Zn_{0.24}Te$ epilayer on a $Cd_{0.76}Zn_{0.24}Te$ substrate (MZT1) and an 11.0 μm $Hg_{0.84}Zn_{0.16}Te$ epilayer on a $Cd_{0.74}Zn_{0.26}Te$ substrate (MZT2). The samples MCT1 and MZT1 are of comparable bandgaps, as are samples MCT2 and MZT2. Table I gives values of hardness versus plastic depth for the four samples. The two HgCdTe epilayer samples range in hardness from 116 kg/mm^2 (1.16 GPa) to 67 kg/mm^2 (0.67 GPa) for x = 0.33 (MCT1) and from 111 kg/mm^2 (1.11 GPa) to 65 kg/mm^2 (0.65 GPa) for x = 0.2 (MCT2).

The hardness depends on plastic depth; smaller depths (i.e., smaller loads) usually give higher hardness values. Vickers hardness measurements were performed on the MCT2 sample since it is sufficiently thick. The average Vickers hardness is 54 kg/mm^2 (0.54 GPa), compared to the Nanoindenter hardness measurements for that sample which range from 111 kg/mm^2 (1.11 GPa) to 65 kg/mm^2 (0.65 GPa). This difference may be explained by the observation that measured hardness typically decreases as the applied load increases (i.e., depth increases) [21]. The Vickers measurements were made using a force of 245 mN (25 g), whereas the largest load applied by the Nanoindenter was approximately 38 mN. This difference may also be due to intrinsic differences in the hardness values measured by the Nanoindenter and the Vickers or Knoop indenters. For soft semiconductors such as CdTe, ZnTe, HgCdTe, and HgZnTe, we see consistently higher hardness values for hardness measured by the Nanoindenter. The hardness values of the MZT1 sample range from 140 kg/mm^2 (1.40 GPa) to 122 kg/mm^2 (1.22 GPa) in one region and from 178 kg/mm^2 (1.78 GPa) to 155 kg/mm^2 (1.55 GPa) in another region. The scatter in the hardness values between two regions on the same sample may be explained by the rough surface and possible compositional variations over the epilayer. The rough surface of the MZT2 sample allowed hardness measurements to be made at only two depths. Since the Nanoindenter is computer controlled, the indentations are programmed and then made automatically. If a sample's surface is not relatively smooth and flat, the Nanoindenter has extreme difficulty in judging the distance from the indenter to the surface and will abort the programmed indentations to protect the indenter. This happened repeatedly with the MZT2 sample. Finally, we programmed each indentation separately, deciding to make only a few indentations at very small and very large depths. The hardness values range from 162 kg/mm^2 (1.62 GPa) to 134 kg/mm^2 (1.34 GPa) at plastic depths of 90 nm and 876 nm, respectively. Since the thinnest epilayer is 7.7 μm thick and the largest indentation depth is 0.905 μm, there is no effect of the ZnCdTe substrates in the measured hardness values. Although there is some difference between the individual HgCdTe samples and the individual HgZnTe samples, these results clearly show that the HgZnTe samples are about twice as hard as the HgCdTe samples of comparable bandgaps. (See figure 8.)

One may calculate "compliance" values from the linear unloading portion of the load versus depth curves of the Nanoindenter tests. Table II gives these compliance values for each effective depth. If the compliance is plotted as a function of the inverse of the effective depth, the result is a straight line whose slope can be used to calculate the Young's modulus for that sample. Figure 9 shows the compliance values versus the 1/effective depth values. The y intercept values, which are a measure of the compliance of the loading column and any additional compliance associated with the mounting of the sample, cluster

around 0.3-3.5 nm/mN, except for the MCT1 sample, whose y intercept is 19.3 nm/mN. This sample was not mounted securely, but this should not affect the validity of the hardness or modulus values since hardness is measured as the indenter encounters resistance. The modulus values are calculated from the slope of the compliance as a function of the inverse of the effective depth, so the intercept value is not important. Table II also gives the calculated values for the Young's modulus for the samples. They measure from 40.0 GPa to 45.7 GPa for the two HgCdTe samples and from 49.0 GPa to 49.3 GPa for the two HgZnTe samples. Simmons and Wang [22] give Young's modulus values of 38.1 GPa for CdTe, 38 GPa for HgTe, and 61.0 GPa for ZnTe. The modulus values for the HgCdTe samples are 13% higher than the expected values for HgCdTe alloys using a linear law relation for the effect of alloying on modulus, while the moduli for the HgZnTe samples are ~16% higher than the expected values for HgZnTe alloys

Two conclusions can be drawn from this work. The HgZnTe samples are twice as hard as the HgCdTe samples of comparable bandgaps. This supports the theoretical work which predicts that HgZnTe is more stable mechanically than HgCdTe. The experimental elastic modulus values for the HgCdTe and HgZnTe samples are very close (only 13-16% higher) to the linearly interpolated values expected from the literature values for the binary compounds.

D. CdTe, ZnTe, and ZnCdTe samples and ZnTe-CdTe superlattices

Another area of activity is the hardness and modulus measurements of thin film and bulk samples of CdTe and ZnTe, of bulk ZnCdTe samples, and of ZnTe-CdTe superlattices. The samples, which are bulk and epilayer ZnTe and CdTe and ZnTe-CdTe superlattices, were measured with the Nanoindenter. The hardness of the bulk ZnCdTe samples was measured using a Vickers indenter. The ZnTe-CdTe superlattices, which consist of 200 cycles of 25 Å of ZnTe or CdTe and 50 Å of ZnTe or CdTe on a 1.0 μm ZnTe buffer layer on a (100) GaAs substrate, were supplied by Dr. David Kisker of AT&T Bell Laboratories. The binary compounds ZnTe and CdTe have a lattice mismatch of 6%, so these are strained layer superlattices. The superlattices were measured in the unannealed and annealed conditions.

Figure 10 shows the hardness of the ZnTe and CdTe epilayer and bulk samples as a function of plastic indentation depth. The hardness values of the ZnTe epilayer and bulk samples are similar and show the same pattern of decreasing hardness with increasing plastic depth. The large increase in hardness at small plastic depths is thought to be due to a surface oxide on these samples, which is evidenced by a discontinuity in the indentation curves at small values of plastic depth. Although the hardness values of the CdTe bulk

sample are lower than those of the epilayer, the CdTe samples do show a similar pattern in hardness. There is no large increase in hardness at very small depths; indentation curves for the CdTe samples show no evidence of a surface oxide being broken. Both epilayer samples show increases in measured hardness at depths > 400 nm as the much harder GaAs substrates begin to influence the data.

Figure 11 shows the hardness of the CdTe-rich and ZnTe-rich superlattices as a function of depth. As is expected (since ZnTe is harder than CdTe), the unannealed and annealed ZnTe-rich superlattices are harder than the corresponding unannealed and annealed CdTe-rich superlattices, respectively. Both unannealed superlattices are harder than the corresponding annealed superlattices, which is due to strengthening from the superlattice structure. Strengthening from multilayers arises from the strain in the layers (compressive in the CdTe layers and tensile in the ZnTe layers) and from different moduli in the layers [23]. Since ZnTe is stiffer than CdTe, dislocations in the CdTe layers are less likely to move into the ZnTe layers unless larger stresses are applied. Both unannealed superlattices show similar patterns in hardness: decreasing hardness with increasing depths in the 400 nm surface region. This pattern is thought to arise from annealing that occurs during the growth of the superlattices. The first ZnTe and CdTe layers interdiffuse to a greater degree since they are at the growth temperature longer. This interdiffusion of the two components decreases the strengthening effects of layers; thus, the hardness values decrease as the indenter reaches the lower layers (i.e., those closer to the buffer layer and substrate).

The annealed superlattices are softer than the corresponding unannealed superlattices, since the strain between layers is diminished due to interdiffusion between layers. Figures 12 and 13 show X-ray diffraction scans of the unannealed and annealed CdTe-rich superlattices, while figures 14 and 15 show XRD scans of the unannealed and annealed ZnTe-rich superlattices. The scans of the two annealed samples show no superlattice sattelite peaks, indicating that the superlattice structure was removed by interdiffusion. There is a difference in the hardness trends for the two annealed superlattices: the hardness of the ZnTe-rich sample is fairly linear with depth while the hardness of the CdTe-rich sample decreases with increasing depth. Upon inspection, however, this apparent difference may be due to a difference in testing: hardness values of the CdTe-rich superlattice range from depths of 18 to 1182 nm, while those of the ZnTe-rich superlattice range from depths of 70 to 1234 nm. Also, the indentation curves at very small depths for the annealed CdTe-rich sample indicate the breaking of a surface oxide. Since the indentation program used did not obtain data for the annealed ZnTe-rich samples at depths < 70 nm, we do not know if this difference in patterns is real.

Figure 16 shows hardness as a function of ZnTe fraction in the bulk ZnCdTe samples and in the ZnTe-CdTe superlattices, as well as hardness values for the epilayer and bulk ZnTe and CdTe samples for reference. Hardness values measured by the Vickers tester and by the Nanoindenter are shown. The lower curve in figure 16 shows Vickers hardness values of ZnCdTe alloys, ranging from 0.5 GPa at 2% ZnTe content to a maximum of 1.0 GPa at 30% ZnTe content. These hardness values show a bowing due to solid solution hardening [24]. This bowing is seen in several ternary semiconductor systems (e.g., HgCdTe [10, 11, 25], InAsP [24], HgZnTe [11, 18, section B]). The hardness values of the binary compounds of CdTe and ZnTe are seen at the endpoints of the curves in figure 16. The hardness values of the epilayers of CdTe and ZnTe, 1.1 GPa and 1.5 GPa, compare favorably to values of the bulk CdTe and ZnTe, 0.8 GPa and 1.4 GPa. These values, however, are higher than Vickers hardness values of bulk CdTe and ZnTe, 0.46 GPa and 0.8 GPa. This difference can be explained by the fact that measured hardness typically increases as the applied load decreases [21]. The Vickers measurements were made using a force of 245 mN (25 g), while the largest load applied by the Nanoindenter at depths of 400 nm was approximately 12 mN. The hardness values measured by the Nanoindenter for our CdTe, ZnTe, HgCdTe, and HgZnTe samples are approximately twice the hardness values measured by either a Vickers indenter or a Knoop indenter. The middle curve in figure 16 shows the hardness of the annealed superlattices. The hardness values of both the CdTe-rich and ZnTe-rich superlattices are 1.7 GPa. If these two values are joined to the hardness values of the binary epilayers, the resulting curve shows a bowing due to solid solution hardening. The upper curve in figure 16 shows the hardness of the unannealed superlattices. The hardness of the CdTe-rich superlattice is 2.2 GPa, while that of the ZnTe-rich superlattice is 2.4 GPa. If these values are connected to the hardness values of the binary epilayers, the resulting curve shows an even more pronounced bowing due to the strengthening by the multilayer structure.

Figure 17 shows Young's modulus values as a function of ZnTe content in the epilayer and bulk ZnTe and CdTe samples and in the superlattices. This figure shows modulus values from the literature [22] and values from the Nanoindenter indentation curves. The lower curve in figure 17 shows calculated modulus values for an isostress model for uniaxial deformation of a (100) multilayer [26]. These moduli for the model are significantly lower than the measured values and the literature aggregate values. (Aggregate modulus values are modulus values for polycrystalline samples with a variety of crystallographic orientations). This suggests that the modulus extracted from the Nanoindenter data is an aggregate value, not a modulus for the crystallographic orientation of the measured sample. The moduli of the binary compounds are seen at the endpoints of the curves in

figure 17. Measured modulus values for the bulk and epilayer CdTe (41.3 GPa and 41.6 GPa, respectively) are very close; however, these values are a little higher than the literature aggregate value (38.1 GPa). Moduli for ZnTe from the literature aggregate value (61.0 GPa) and from the measured bulk (61.3 GPa) and epilayer (61.8 GPa) values are extremely close. The middle curve in figure 17 shows modulus values of the annealed superlattices. The modulus of the CdTe-rich superlattice is 49.8 GPa, while that of the ZnTe-rich superlattice is 52.5 GPa. If these values are joined to the moduli of the binary epilayers, the resulting curve shows a linear increase with increasing ZnTe fraction due to alloying. The upper curve in figure 17 shows moduli of the unannealed superlattices. The modulus of the CdTe-rich superlattice is 51.0 GPa, while that of the ZnTe-rich superlattice is 61.2 GPa. If these values are joined to the moduli of the binary epilayers, the resulting curve shows a slight bowing due to the strain in the multilayers.

Several important conclusions can be made from these experiments. Increases in hardness in both ZnCdTe samples and annealed superlattices due to solid solution hardening were found. Increases in hardness with increasing ZnTe content in the unannealed superlattices, as compared to the corresponding annealed superlattices, were found. Layering effects arising from strains in the layers and from different moduli in the layers cause these increases in hardness. Hardness values of bulk ZnTe and CdTe show reasonable agreement with hardness values of epilayer ZnTe and CdTe. A linear increase in modulus values with increasing ZnTe content of annealed superlattices is due to alloying and a slight increase (beyond the linear increase) in moduli of unannealed superlattices is due to the superlattice structure. Modulus values of bulk and epilayer samples of ZnTe and CdTe agree with each other and with literature aggregate moduli for ZnTe and CdTe. The modulus value measured by the Nanoindenter appears to be an aggregate modulus.

E. Hardness studies in AlGaAs and GaInSb

We have measured the hardness of two $Al_xGa_{1-x}As$ films (where x = 0.30 and 0.35) and a GaAs substrate using the Nanoindenter. The AlGaAs films were deposited on GaAs substrates by molecular beam epitaxy (MBE) by Dr. Martin Scott of Hewlett Packard and are ~3000 Å thick. Figure 18 shows these measurements. The results are unexpected for a number of reasons. The hardness values increase with increasing depth, contrary to the usual obervation of decreasing hardness with increasing applied load (i.e., increasing depth). Also, both AlGaAs films are expected to be softer than the GaAs sample, since GaAs is ~27% harder than literature values for AlAs [24]. While the hardness values of the $Al_{0.35}Ga_{0.65}As$ film are practically identical to those of the GaAs sample, the $Al_{0.3}Ga_{0.7}As$ film is 13% harder than the GaAs sample. The $Al_{0.35}Ga_{0.65}As$ film shows the expected

behavior for a film on a harder substrate; namely, as the indentation depth increases, an increase in hardness is observed because of the harder substrate. The $Al_{0.3}Ga_{0.7}As$ film shows an unexpected behavior, since its hardness is fairly constant with depth and no substrate effect is seen.

The pseudobinary semiconductor, $Ga_xIn_{1-x}Sb$, was chosen for bulk growth because the melting temperature is fairly low and because there is information in the literature on the growth of this system arising from an interest in its use for Gunn devices and three-level oscillators [27]. Single crystal growth of $Ga_xIn_{1-x}Sb$ is difficult because of the high segregation of GaSb in InSb, interface breakdown due to constitutional supercooling, and low diffusion rates in the material [28]; however, we have obtained coarse grained samples of varying composition suitable for microhardness measurements. Bulk samples were grown by a vertical Bridgman technique using an encapsulated crucible. The liquid was homogenized by a five day anneal and growth was made at a 0.8 mm/day rate. The ingot was then removed and sectioned. The ingots are polycrystalline with long columnar grains (some as long as 15-20 mm) about 2-4 mm in diameter. Microprobe analysis was performed on the ingots and Vickers hardness measurements were made. Figure 19 shows hardness versus composition in $Ga_xIn_{1-x}Sb$. The figure also shows literature values [24] for the two binary semiconductors and three ternary alloy samples. The load applied during testing can cause a difference in hardness measurements, so we are careful to compare values taken at the same load (100 g). The results are interesting--our hardness values show no strengthening in the ternary alloys, other than that predicted by a linear hardening law. The bowing of the hardness curve seen by Goryunova et al. [24] is not seen in our data.

F. Factors influencing hardness values

When we started compiling hardness data on semiconductors from the literature, we noticed a wide range of hardness values for many semiconductors. There are several possible reasons for this wide variety: (1) differences in hardness of different grains, across twins, and as the sample is rotated due to crystal orientation effects; (2) differences in hardness depending upon illumination during testing arising from the photoplastic effect in certain semiconductors; and (3) differences in hardness arising from differences in applied loads during hardness testing. We have examined these effects (see tables III and IV and figure 20) and found that none of them appears to strongly influence Vickers hardness in the systems we studied.

Figure 21 shows hardness values from the literature versus bond length at 300 K for many binary and elemental semiconductors. As can be seen, there is a wide range in

the reported values. This wide range in hardness values is a problem when one is searching for meaningful hardness values in semiconductors.

IV. Proposed work

We have made significant progress in studying the hardness and modulus of compound semiconductors and we propose to continue this work. Studies will be predominantly on thin films for a number of reasons. Most semiconductor alloys cannot be grown as bulk samples, but can be grown as thin films. Furthermore, thin films are the form usually used in practice. The most effective tool for these studies is the Nanoindenter.

A. Superlattices

Semiconductor superlattices are of theoretical and practical interest since bandgaps can be finely tuned by the proper choice of the semiconductor materials and layer thicknesses. Bedair et al. [29] have reported using GaAsP-InGaAs strained layer superlattices to reduce threading dislocations orginating from GaAs substates. The GaAs epilayers grown on these superlattice buffers were found to be almost dislocation-free. Gourley et al. [30] have also reported success in using strained layer InGaAs-InAlAs superlattices to filter dislocations. Despite the interest in superlattices as filters to reduce the dislocation density of epilayers and as devices, very little work has been done on the mechanical properties of superlattices. The main problem, of course, is the small size and thickness of these samples. However, with the use of the Nanoindenter, meaningful data on hardness and elastic modulus can be obtained. These data, along with cross section TEM data, should yield important information on the way dislocations interact with the interfaces of the layers and on the effects of the strain within layers on dislocation motion.

We have ZnTe-CdTe superlattice samples of varying ZnTe content over a broader composition that can add to our present data on hardness and elastic moduli. We propose to do cross section TEM studies of the unannealed and annealed superlattices to obtain details about the dislocation structure of the multilayers, which could help to explain both the dislcation filtering and the strengthening effect of multilayers.

We are collaborating with Dr. Art Clawson of the Naval Ocean Systems Center who can supply us with superlattices of InGaAsP. Dr. Clawson has already provided us with strained layer InGaAs-InAsP superlattices and plans to grow lattice matched $In_{0.53}Ga_{0.47}As$-InP superlattices. Hardness and moduli (measured by the Nanoindenter), X-ray diffraction scans, and cross section TEM studies will be used to characterize these

superlattices, both unannealed and annealed. Of particular interest is the role of strain in the dislocation filtering and strengthening effect of multilayers. Since we will examine samples of both strained layer and lattice matched superlattices of the InGaAsP system, we can study the role of strain in these samples. We also propose to investigate Si-Ge superlattices in order to expand our study over the three families of superlattices--III-V, II-VI, and IV-IV superlattices.

B. Creep tests

We propose to study creep in semiconductors of relatively low melting temperatures. The study of semiconductors of low melting temperatures arises from the fact that the currently available Nanoindenter can be used only at room temperature and creep tests are typically run at 40-60% of the melting temperature of the materials. We have performed a sample creep test on a HgTe sample by loading a Vickers hardness indenter overnight and then observing the indentation with time. The sample did show a 31% decrease in measured hardness in this rough test, an indication that creep did occur. Creep tests run on the Nanoindenter will provide more information. By examining creep behavior in materials, we will gain important information about dislocation behavior in the samples. Solid solution metallic alloys behave either as Class I or Class II alloys [31]. In Class I alloys, dislocation motion is controlled by glide, while, in Class II alloys, dislocation motion is controlled by climb or by jogged screw dislocations. It will be informative to compare the information that can be obtained from the Nanoindenter creep tests to what is already known about dislocation motion in semiconductors.

C. Growth techniques

Time and resources permitting, we will use two techniques for preparing samples: thick films by ISOVPE and bulk samples by the vertical Bridgman method. The ISOVPE method was effective for growing thick films of HgCdTe on CdTe substrates and thick films of HgZnTe on ZnTe substrates. We propose to investigate using the ISOVPE method to grow films of other ternary semiconductors. The limitations are the lattice mismatch and the relative vapor pressure of the two component binaries. Possible semiconductor systems that may be grown by the method are: ZnTe-CdTe; HgTe-GeTe; GeTe-PbTe; GaP-InP; GaAs-InAs; GaP-GaAs; and InP-InAs. Table V lists the lattice mismatch and the melting temperatures for the candidate systems. The systems with the smaller lattice mismatch should produce epilayers of higher quality than those with larger lattice mismatch. We will explore the method with the most promising of these systems,

and, if good quality films of sufficient thickness can be grown, microhardness measurements will be made as a function of composition.

We were successful in using the vertical Bridgman method with the GaInSb system to grow coarse grained samples suitable for hardness measurement and we believe that we can use this method for other pseudobinary semiconductors. The main limitation of our vertical Bridgman equipment for this purpose is the need for fairly low melting temperatures and low decomposition vapor pressures. For semiconductor systems with high melting temperatures and decomposition pressures, special high pressure growth systems are needed.

V. Summary

We have reported on progress in five major areas: (1) the preparation and hardness measurement of HgCdTe epilayers on CdTe substrates; (2) the growth and the measurement of hardness and interdiffusion coefficients of HgZnTe of different compositions on ZnTe substrates; (3) the measurement of hardness and elastic modulus of HgCdTe and HgZnTe epilayers grown on ZnCdTe substrates; (4) the measurement of hardness and elastic modulus of epilayer and bulk samples of ZnTe and CdTe, and of unannealed and annealed ZnTe-CdTe superlattices; and (5) the growth and hardness measurement of GaInSb.

We propose to continue this work by using the Nanoindenter: (1) to continue our work on the ZnTe-CdTe superlattices; (2) to investigate both strained layer and lattice matched samples of the III-V superlattices of InGaAsP; (3) to investigate superlattices of Si and Ge; and (4) to run creep tests on HgTe samples and other semiconductors of relatively low melting temperatures. Time and resources permitting, we will also investigate two growth techniques: (1) the ISOVPE method to grow other ternary semiconductors and (2) the vertical Bridgman method to grow coarse grained ingots of selected ternary semiconductors.

References

1. A. Sher, A.-B. Chen, W. E. Spicer, and C. Shih, in Proceedings of the 1984 U.S. Workshop on the Physics and Chemistry of Mercury Cadmium Telluride: American Vacuum Society and American Institute of Physics, T. Casselman, editor (1985).

2. M. C. Flemings, Solidification Processing, McGraw Hill (1973) p. 64.

3. W. W. Mullins and R. F. Sekerka, J. Appl. Phys., 34, 323 (1963); 35, 444 (1964).

4. R. F. Sekerka, J. Appl. Phys., 36, 264 (1965).

5. R. F. Sekerka, J. Phys. Chem. Solids, 28, 983 (1967).

6. R. F. Sekerka, J. Crystal Growth, 3, 71 (1968).

7. M. F. Doerner and W. D. Nix, J. Mater. Res., 1, 601 (1986).

8. Y. Marfaing, G. Cohen-Solal, and F. Bailly, in Proceedings of an International Conference on Crystal Growth, Boston, 20-24 June 1966, H. S. Peiser, editor.

9. J. G. Fleming, Ph.D. Thesis, Stanford University, 1986.

10. S. Cole, M. Brown, and A. F. W. Willoughby, J. Mat. Sci., 17, 2061 (1982); 20, 274 (1985).

11. R. Triboulet, A. Lasbley, B. Toulouse, and R. Granger, J. Crystal Growth, 79, 695 (1986).

12. I. V. Kurilo, I. M. Spitkovskii, and A. D. Schneider, Izv. VUZ Fiz., 9, 130 (1974).

13. B. B. Sharma, S. K. Mehta, and V. V. Agashe, Phys. Stat. Sol. (a), 60, K105 (1980).

14. B. P. Koman and M. V. Pashovskii, Ukr. Fiz. Zh., 23, 58 (1978).

15. J. F. Barbot, F. Rivard, and J. C. Desoyer, J. Mat. Sci., 23, 163 (1988).

16. A. Sher, A.-B. Chen, W. E. Spicer, and C.-K. Shih, J. Vac. Sci. Technol., A3, 105 (1985).

17. C. Pobla, R. Granger, S. Rolland, and R. Triboulet, J. Crystal Growth, 79, 515 (1986).

18. M. Schenk and A. Fissel, J. Crystal Growth, 86, 502 (1988).

19. J. G. Fleming and D. A. Stevenson, Phys. Stat. Sol. (a), 105, 77 (1987).

20. S. Fang, L. J. Farthing, M. F. S. Tang, and D. A. Stevenson, to be published in J. Vac. Sci. Technol., March/April 1990.

21. D. Tabor, in Microindentation Techniques in Materials Science and Engineering ASTM STP 889, P. J. Blau and B. R. Lawn, editors (1986) pp. 125-159.

22. G. Simmons and H. Wang, Single Crystal Elastic Constants and Calculated Aggregate Properties: A Handbook, 2nd ed., The M.I.T. Press, Cambridge (1971).

23. M. F. Doerner, Ph.D. Thesis, Stanford University, 1987.

24. N. A. Goryunova, A. S. Borshchevskii, and D. N. Tretiakov, in Semiconductors and Semimetals, vol. 4, Physics of III-V Compounds, R. K. Willardson and A. C. Beer, editors, (1968) pp. 3-34.

25. J. G. Fleming, L. J. Farthing, and D. A. Stevenson, J. Crystal Growth, 86, 506 (1988).

26. W. D. Nix (private communication).

27. A. Joullie, P. Esquirol, and G. Bougnot, Mat. Res. Bull., 9, 641 (1974).

28. A. Joullie, J. Allegre, and G. Bougnot, Mat. Res. Bull., 7, 1101 (1972).

29. S. M Bedair, T. P. Humphreys, N. A. El-Masry, Y. Lo, N. Hamaguchi, C. D. Lamp, A. A. Tuttle, D. L. Dreifus, and P. Russell, Appl. Phys. Lett. 49, 942 (1986).

30. P. L. Gourley, T. J. Drummond, and B.L. Doyle, Appl. Phys. Lett., 49, 1101 (1986).

31. W. R. Cannon and O. D. Sherby, Met. Trans, 1, 1030 (1970).

Presentations and Publications

1. E. J. Smith, S. Sen, M. T. Smith, C. R. Curtis, L. J. Farthing, T. Weihs, M. F. S. Tang, and D. A. Stevenson, "Growth and Characterizaion of Bulk and Epitaxial HgZnTe," paper presented at the Infrared Industries Symposium, National Bureau of Standards, Gaithersburg, Maryland, June 9-10, 1987.

2. E. J. Smith, S. Sen, M. T. Smith, C. R. Curtis, L. J. Farthing, T. Weihs, M. F. S. Tang, and D. A. Stevenson, "Growth and Characterizaion of Bulk and Epitaxial HgZnTe," Proceedings from the Infrared Industries Symposium, National Bureau of Standards, Gaithersburg, Maryland, June 9-10, 1987.

3. E. J. Smith, S. Sen, M. T. Smith, C. R. Curtis, M. F. S. Tang, T. Weihs, L. J. Farthing, and D. A. Stevenson, "Growth and Characterizaion of Bulk and Epitaxial HgZnTe," paper presented at the Seventh American Conference on Crystal Growth, July 12-17, 1987, Monterey, California.

4. J. G. Fleming, L. J. Farthing, and D. A. Stevenson, "Vickers Hardness of $Hg_{1-x}Cd_xTe$ Epilayers Grown by Isothermal Vapor Phase Epitaxy," poster presented at the Seventh American Conference on Crystal Growth, July 12-17, 1987, Monterey, California.

5. J. G. Fleming, L. J. Farthing, and D. A. Stevenson, "Vickers Hardness of $Hg_{1-x}Cd_xTe$ Epilayers Grown by Isothermal Vapor Phase Epitaxy," J. Crystal Growth, 86, 506 (1988).

6. L. J. Farthing, T. P. Weihs, D. W. Kisker, J. J. Krajewski, M. F. S. Tang, and D. A. Stevenson, "Hardness and Elastic Modulus Measurements in CdTe and ZnTe Thin Film and Bulk Samples and ZnTe-CdTe Superlattices," paper presented at the Materials Research Society Fall Meeting 1988, Boston, Massachusetts.

7. L. J. Farthing, T. P. Weihs, D. W. Kisker, J. J. Krajewski, M. F. S. Tang, and D. A. Stevenson, "Hardness and Elastic Modulus Measurements in CdTe and ZnTe Thin Film and Bulk Samples and ZnTe-CdTe Superlattices," Materials Research Society, Thin Films: Stresses and Mechanical Properties, vol. 130, 1989.

8. L. J. Farthing, T. P. Weihs, D. W. Kisker, J. J. Krajewski, M. F. S. Tang, and D. A. Stevenson, "Mechanical Properties Studies of CdTe-ZnTe Superlattices," paper presented at the American Association for Crystal Growth/West, Eleventh Conference on Crystal Growth, June 5-8, 1989, Fallen Leaf Lake, California.

9. S. Fang, L. J. Farthing, M. F. S. Tang, and D. A. Stevenson, "Diffusion and Hardness Studies in Mercury Zinc Telluride," paper presented at the 1989 U.S. Workshop on the Physics and Chemistry of Mercury Cadmium Telluride and Related II-VI Compounds, Oct. 3-5, 1989, San Diego, California.

10. S. Fang, L. J. Farthing, M. F. S. Tang, and D. A. Stevenson, "Diffusion and Hardness Studies in Mercury Zinc Telluride," to be published in J. Vac. Sci. Technol., March/April 1990.

Table I. Hardness as a function of plastic depth for MCT and MZT epilayers

Sample	$H_{plastic}$ (nm)	Hardness (GPa)	Hardness (kg/mm^2)
$Hg_{0.67}Cd_{0.33}Te$ epilayer on $Cd_{0.96}Zn_{0.04}Te$ substrate (MCT1)	86.6	1.159	116
	170.9	1.003	100
	405.2	0.796	80
	763.9	0.672	67
$Hg_{0.8}Cd_{0.2}Te$ epilayer on $Cd_{0.96}Zn_{0.04}Te$ substrate (MCT2)	92.9	1.108	111
	185.3	0.966	97
	461.9	0.787	79
	905.1	0.644	64
$Hg_{0.76}Zn_{0.24}Te$ epilayer on $Cd_{0.76}Zn_{0.24}Te$ substrate (MZT1)	92.8	1.396	140
	185.8	1.251	125
	452.7	1.310	131
	885.6	1.221	122
	87.9	1.779	178
	87.7	1.783	178
	178.8	1.615	162
	440.1	1.567	157
	839.1	1.555	156
	853.9	1.552	155
$Hg_{0.84}Zn_{0.16}Te$ epilayer on $Cd_{0.74}Zn_{0.26}Te$ substrate (MZT2)	89.5	1.619	162
	875.8	1.338	134

a

Table II. "Compliance" as a function of effective depth and Young's modulus values for MCT and MZT epilayers

Sample	$H_{effective}$ (nm)	"Compliance" (nm/mN)	Young's modulus (GPa)
$Hg_{0.67}Cd_{0.33}Te$ epilayer on $Cd_{0.96}Zn_{0.04}Te$ substrate (MCT1)	113.6	53.63	40.0
	201.6	39.16	
	437.9	28.94	
	785.5	25.00	
$Hg_{0.8}Cd_{0.2}Te$ epilayer on $Cd_{0.96}Zn_{0.04}Te$ substrate (MCT2)	120.0	34.37	45.7
	215.6	20.75	
	493.5	10.86	
	920.9	7.69	
$Hg_{0.76}Zn_{0.24}Te$ epilayer on $Cd_{0.76}Zn_{0.24}Te$ substrate (MZT1)	119.8	28.39	50.6
	216.1	15.90	
	484.4	7.13	
	902.2	4.11	
	114.8	32.19	47.4
	114.6	31.06	
	209.3	17.12	
	472.1	7.65	
	857.6	5.13	
	871.8	4.31	
$Hg_{0.84}Zn_{0.16}Te$ epilayer on $Cd_{0.74}Zn_{0.26}Te$ substrate (MZT2)	116.4	30.28	49.3
	852.7	4.72	

Table III. The effect of grains and twins on Vickers hardness

Sample	Grain or twin	Vickers hardness (kg/mm^2)
$Zn_{0.02}Cd_{0.98}Te$	twin #1	55.7 (2.0)*
	twin #2	56.9 (1.3)
	grain #1	54.8 (3.5)
	grain #2	54.4 (2.7)
$Zn_{0.04}Cd_{0.96}Te$	grain #1	60.7 (1.4)
	grain #2	60.3 (0.9)
CdTe sample #1	twin #1	48.4 (2.1)
	twin #2	44.4 (1.0)
CdTe sample #2	twin #1	47.0 (0.8)
	twin #2	42.3 (1.0)
In-doped CdTe sample #1	twin #1	50.0 (1.6)
	twin #2	44.7 (0.8)
In-doped CdTe sample #2	twin #1	49.3 (1.1)
	twin #2	43.3 (0.6)

* The standard deviation of the data is in parenthesis.

Table IV. The effect of lighting on Vickers hardness

Sample	Lighting	Vickers hardness (kg/mm^2)
CdTe sample #1	normal lab	50.3 (0.5)*
	lamps at lowest setting[1]	53.0 (0.2)
	lamps at medium setting	53.0 (0.4)
	lamps at highest setting	53.3 (0.7)
CdTe sample #2	normal lab	50.0 (1.4)
	darkness	49.2 (0.7)
$Zn_{0.04}Cd_{0.96}Te$ sample #1	normal lab	63.4 (0.1)
	lamps at medium setting	65.3 (0.9)
$Zn_{0.04}Cd_{0.96}Te$ sample #2	normal lab	61.1 (1.5)
	lamps at highest setting	59.5 (0.9)
	darkness	60.7 (1.1)
$Hg_{0.8}Cd_{0.2}Te$	normal lab	34.6 (0.7)
	darkness	33.5 (0.7)

* The standard deviation of the data is in parenthesis.

1 The lamps are 10^{-3} watts/cm^2 at the highest setting.

d

Table V. Lattice mismatch and melting temperatures of selected III-V and II-VI systems

System	% Lattice Mismatch	Melting Temperature (K)
ZnTe-CdTe	6.1	ZnTe 1568 CdTe 1365
HgTe-PbTe	0.3	HgTe 943 PbTe 1180
HgTe-GeTe	7.1	HgTe 943 GeTe 998
GeTe-PbTe	7.4	GeTe 998 PbTe 1180
GaP-InP	7.4	GaP 1750 InP 1330
GaAs-InAs	7.0	GaAs 1510 InAs 1215
GaP-GaAs	3.7	GaP 1750 GaAs 1510
InP-InAs	3.2	InP 1330 InAs 1215

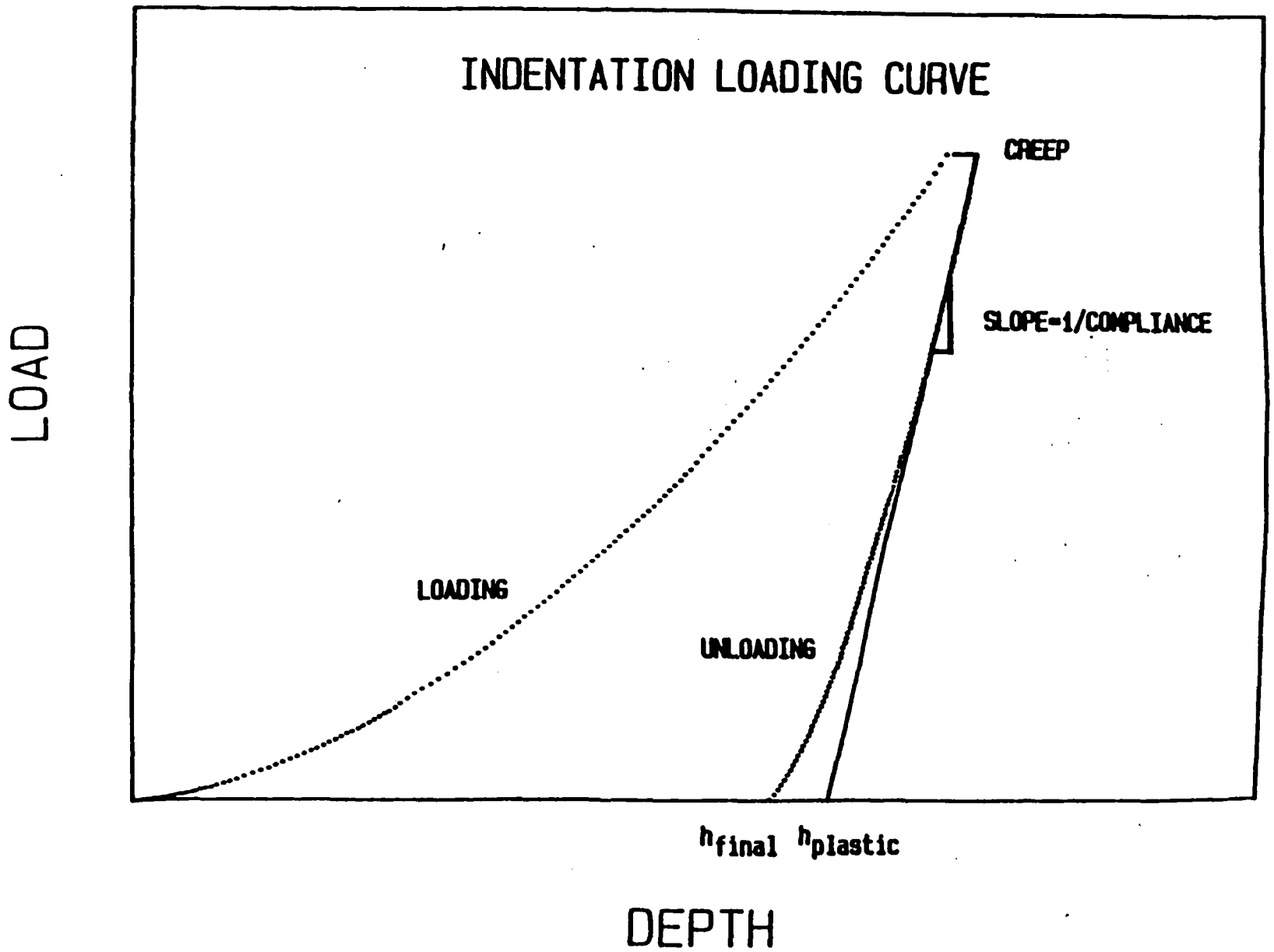

Figure 1. A typical indentation curve from the Nanoindenter showing load versus depth.

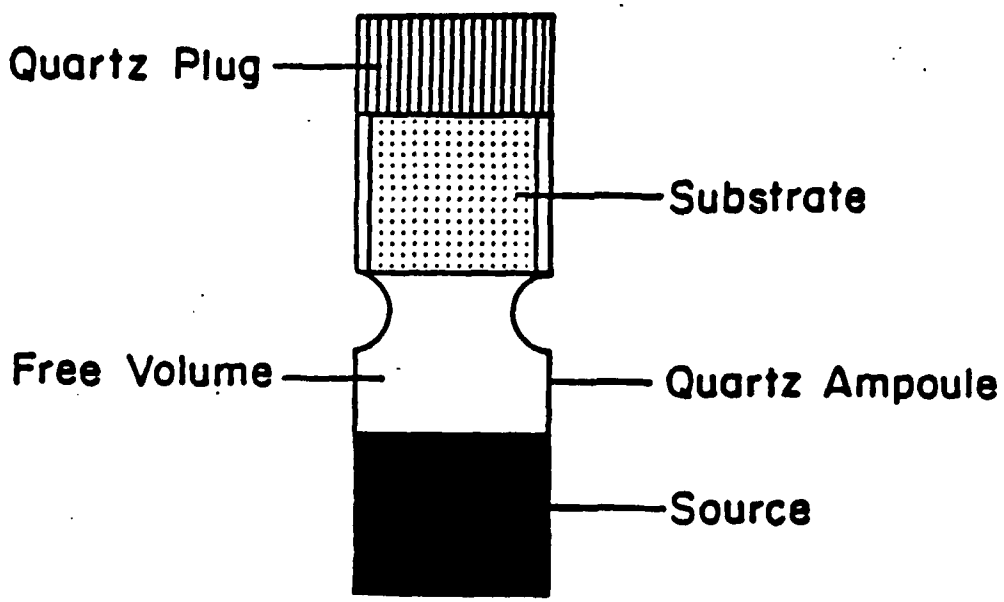

Figure 2. The geometry used in the ISOVPE experiments. Different points on the substrate are different distances from the source, which causes a gradient in composition.

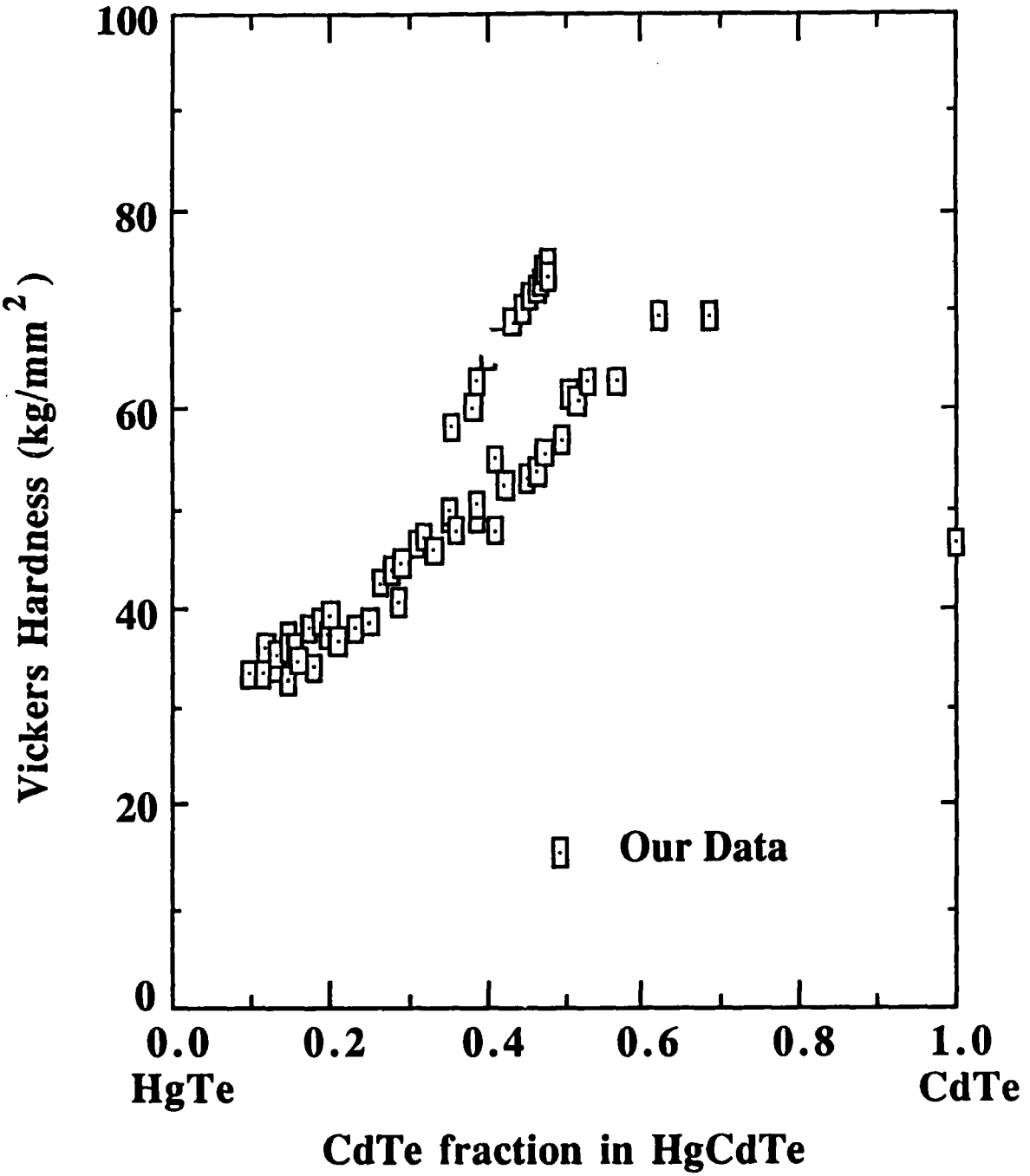

Figure 3. Vickers hardness as a function of CdTe fraction in HgCdTe

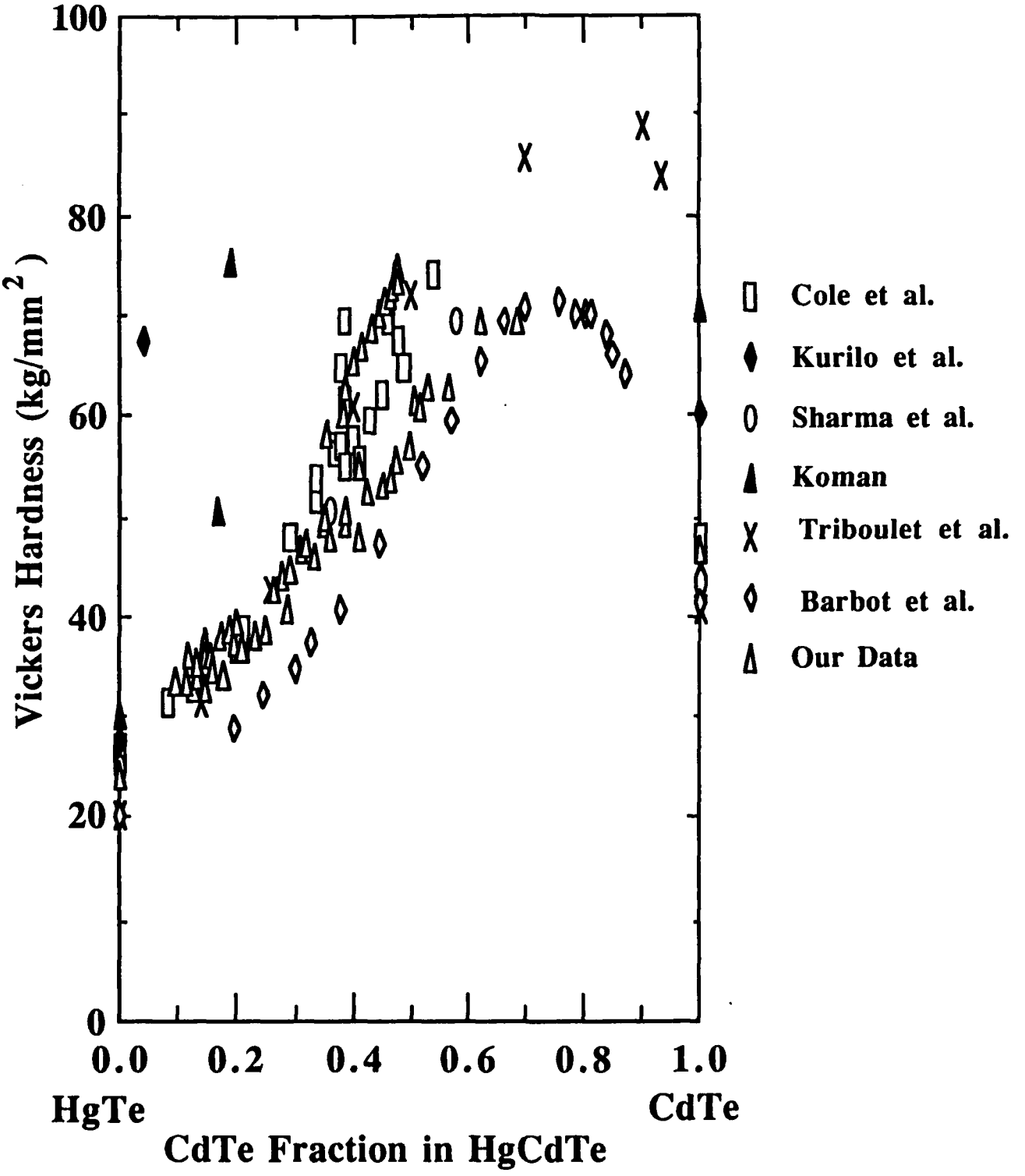

Figure 4. Vickers hardness versus CdTe fraction in HgCdTe for our data and data from the literature

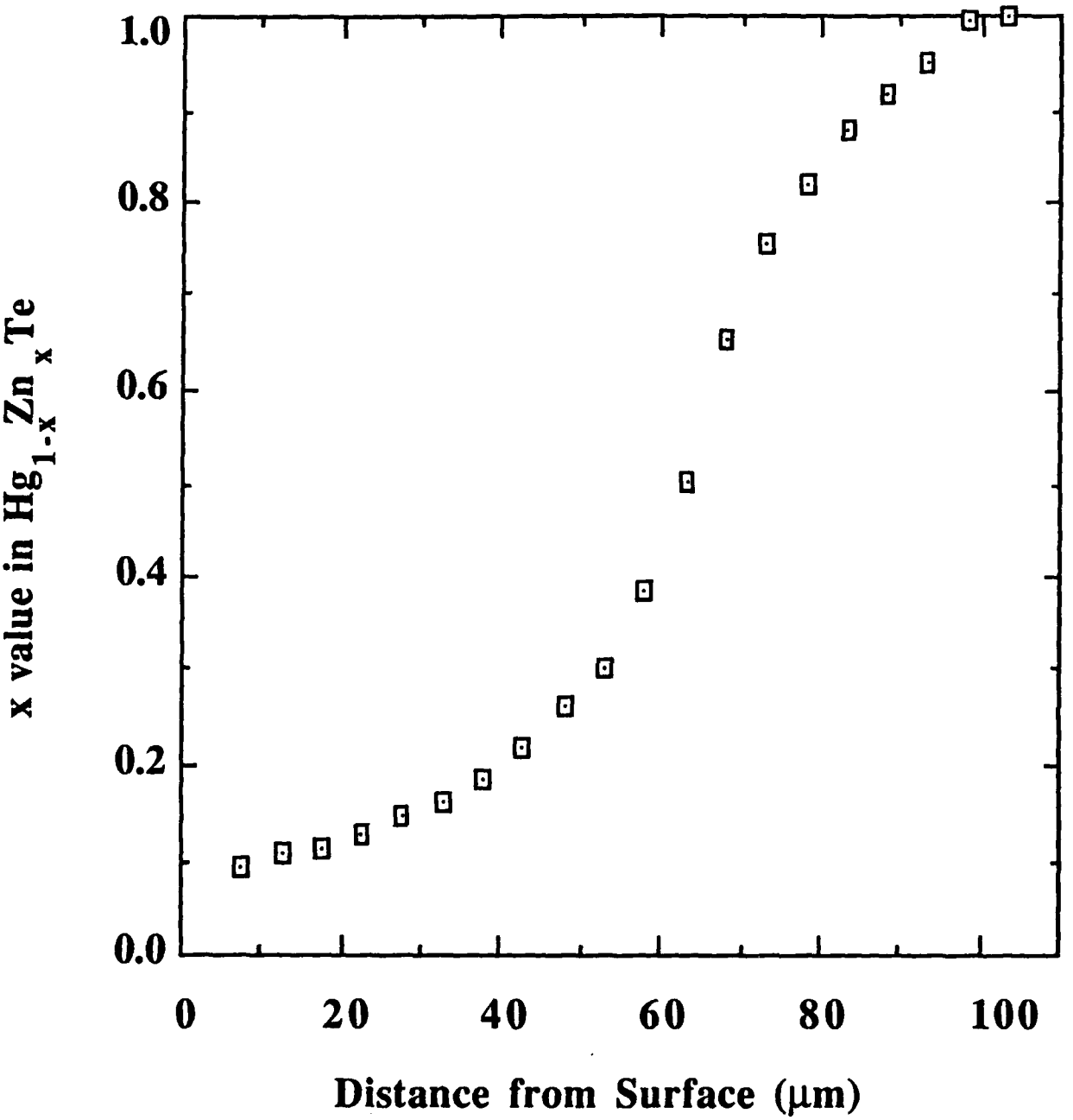

Figure 5. Typical concentration profile for ISOVPE HgZnTe epilayer (550°C, 48 hr.)

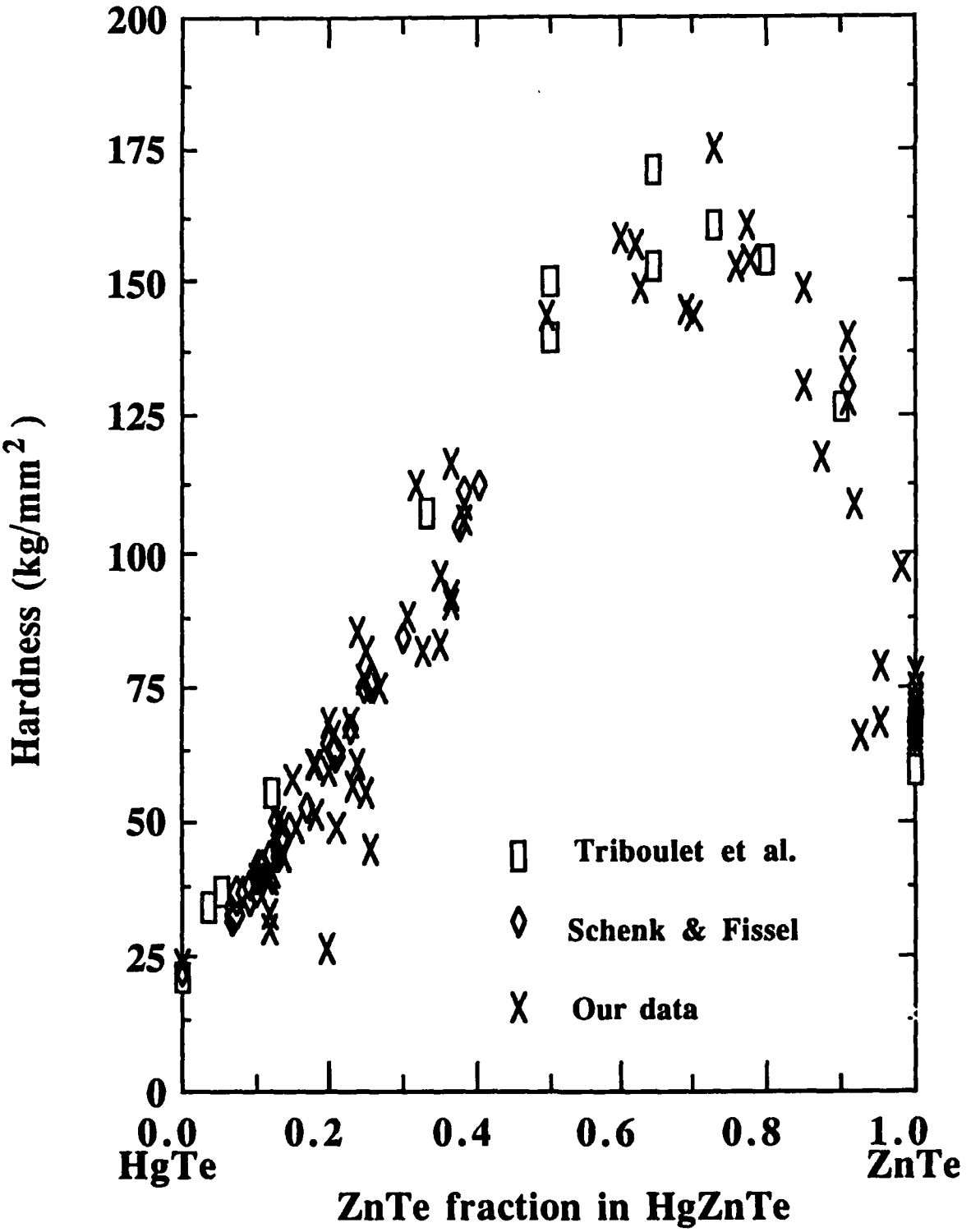

Figure 6. Hardness versus ZnTe fraction in HgZnTe for our data and data from the literature

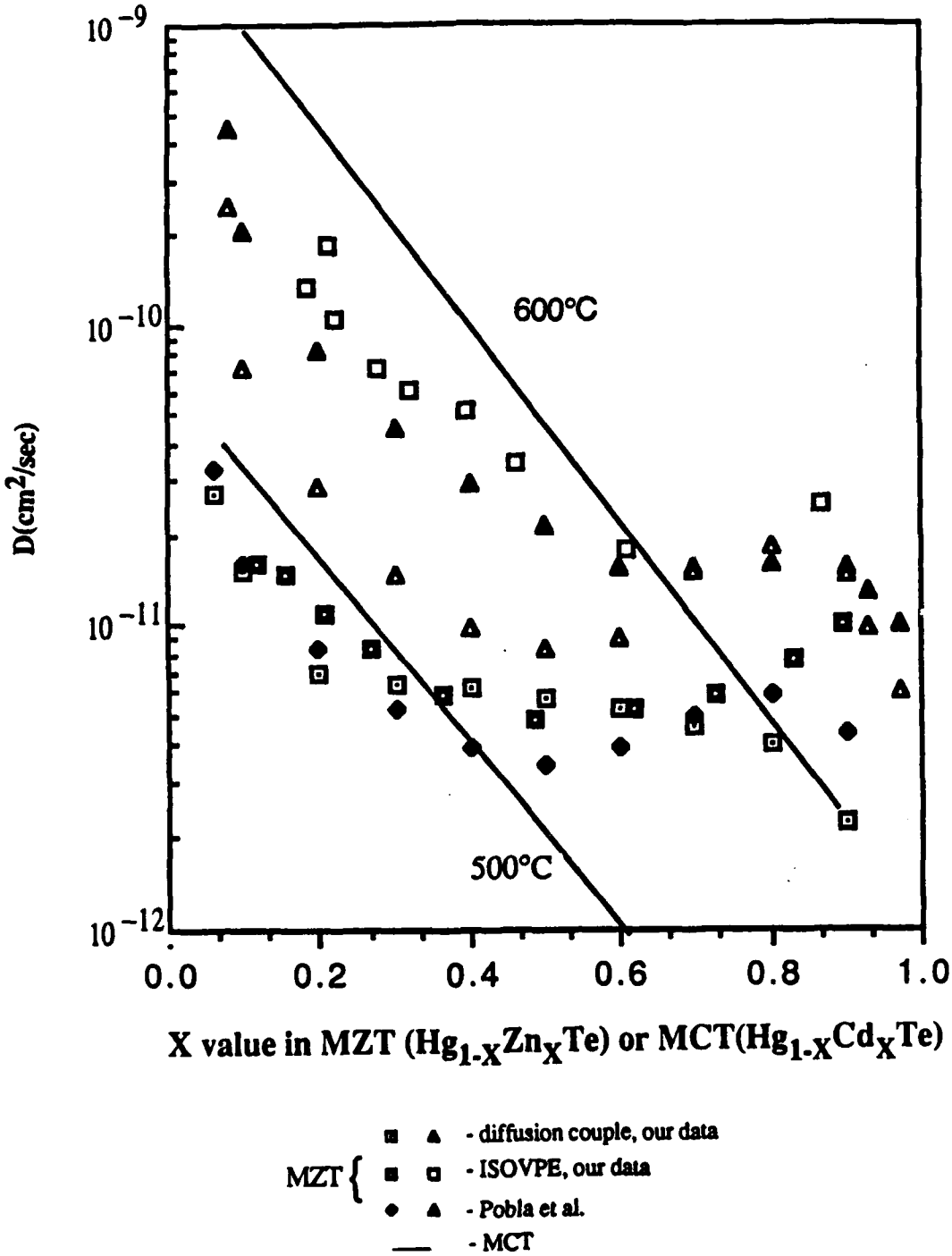

Fig. 7. Interdiffusion coefficients of MZT and MCT

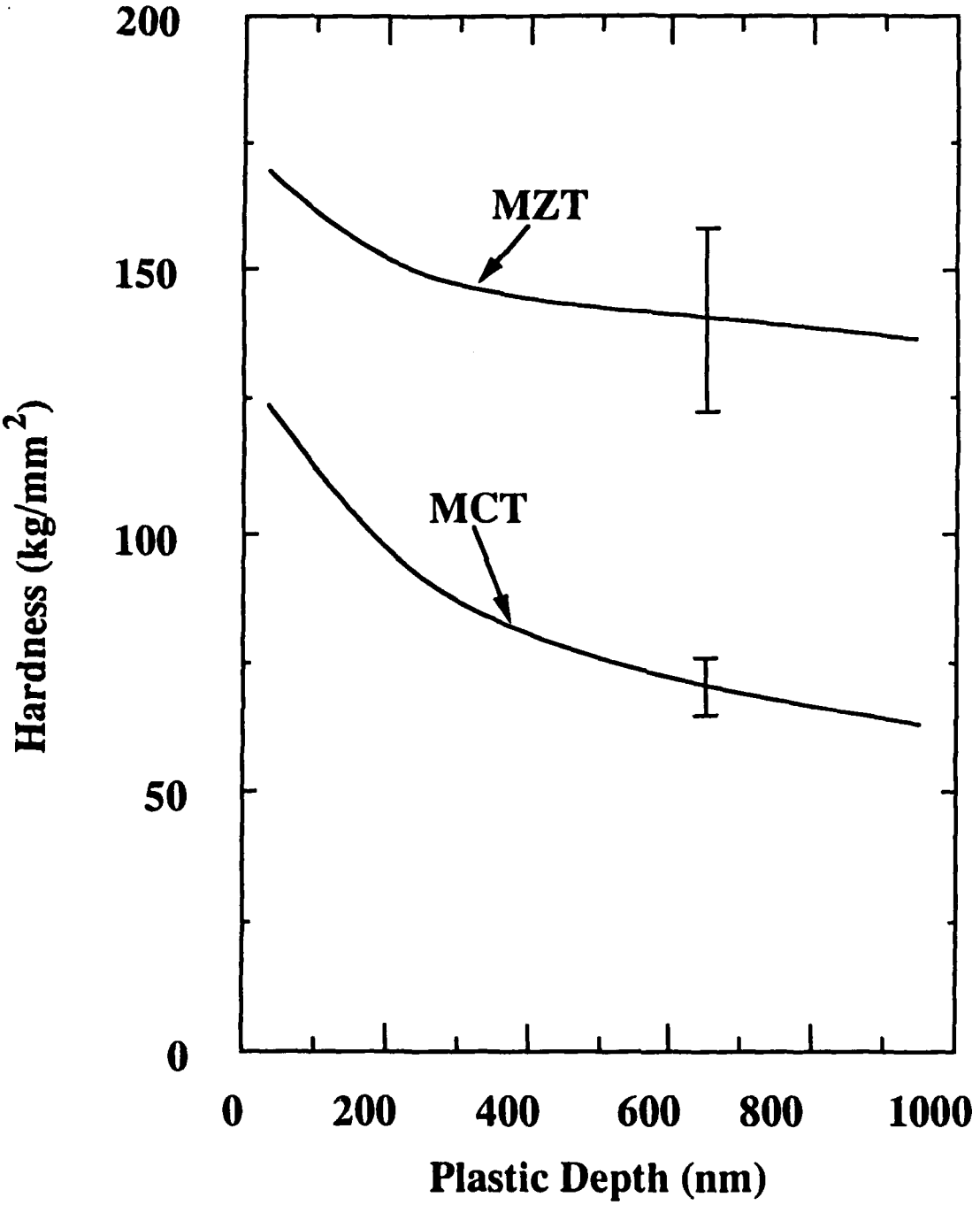

Figure 8. Hardness of HgCdTe and HgZnTe epilayers as a function of plastic depth

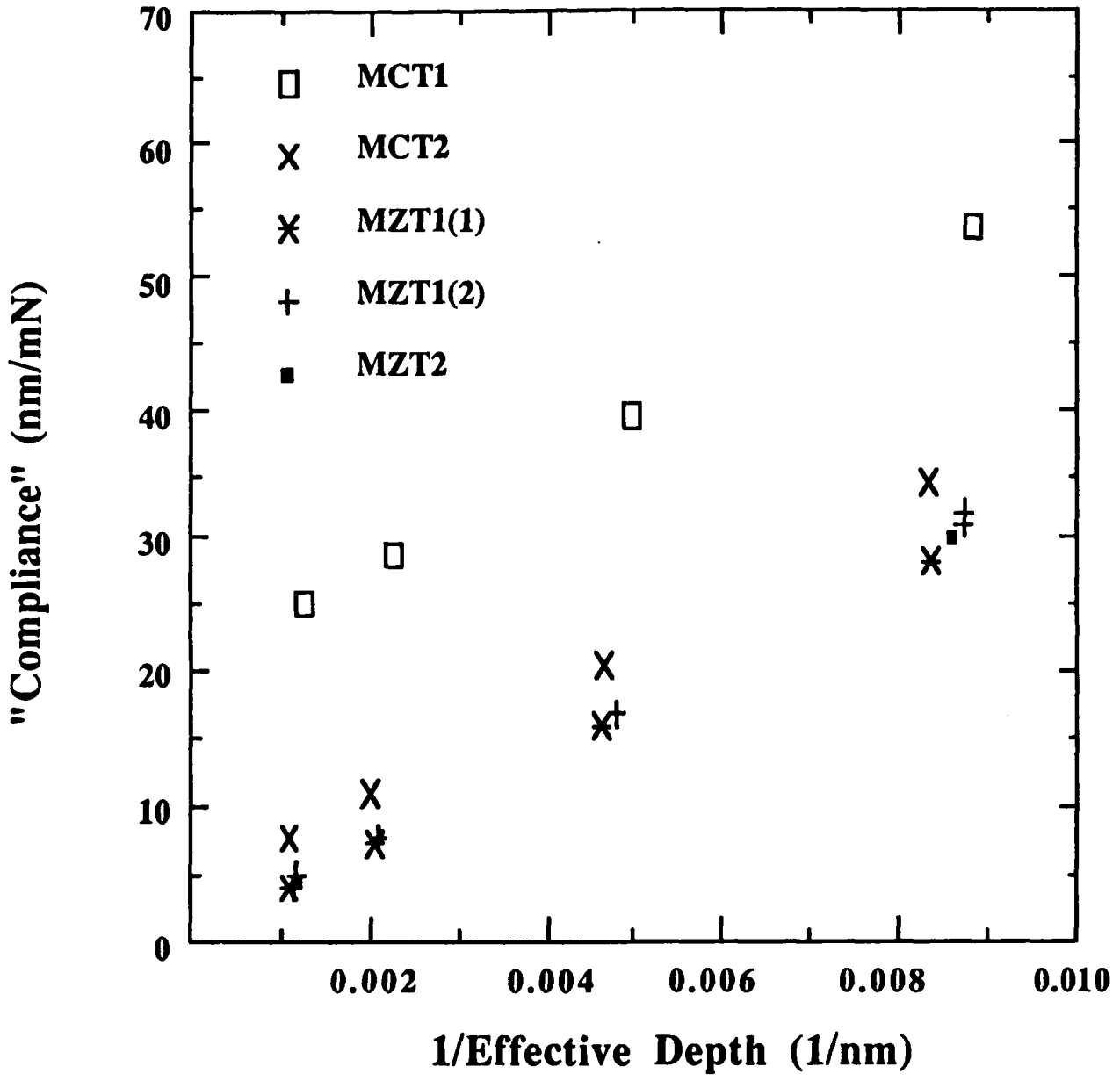

Figure 9. "Compliance" versus inverse effective depth for the MCT and MZT samples

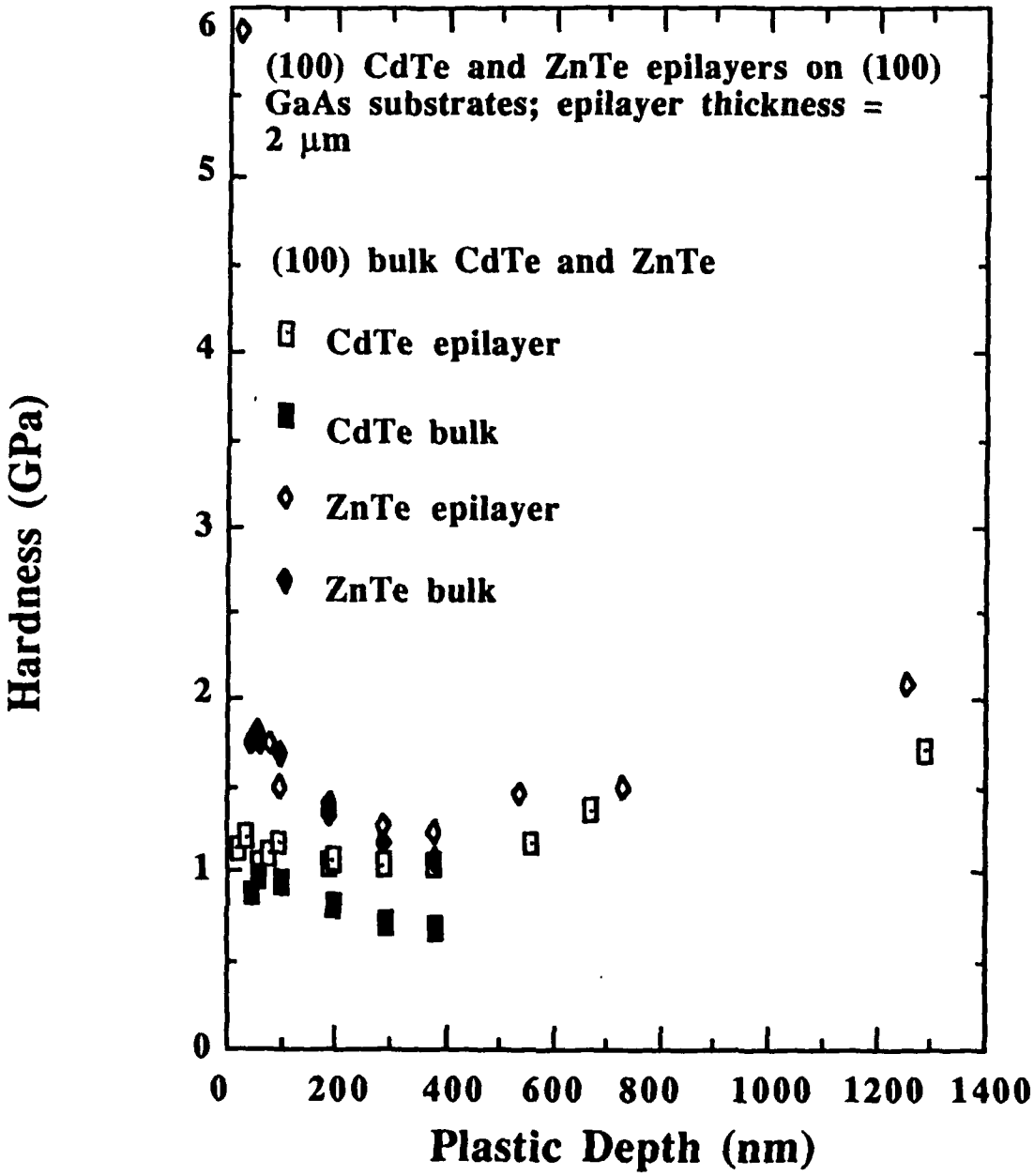

Figure 10. Hardness of epilayer and bulk ZnTe and CdTe samples as a function of plastic depth

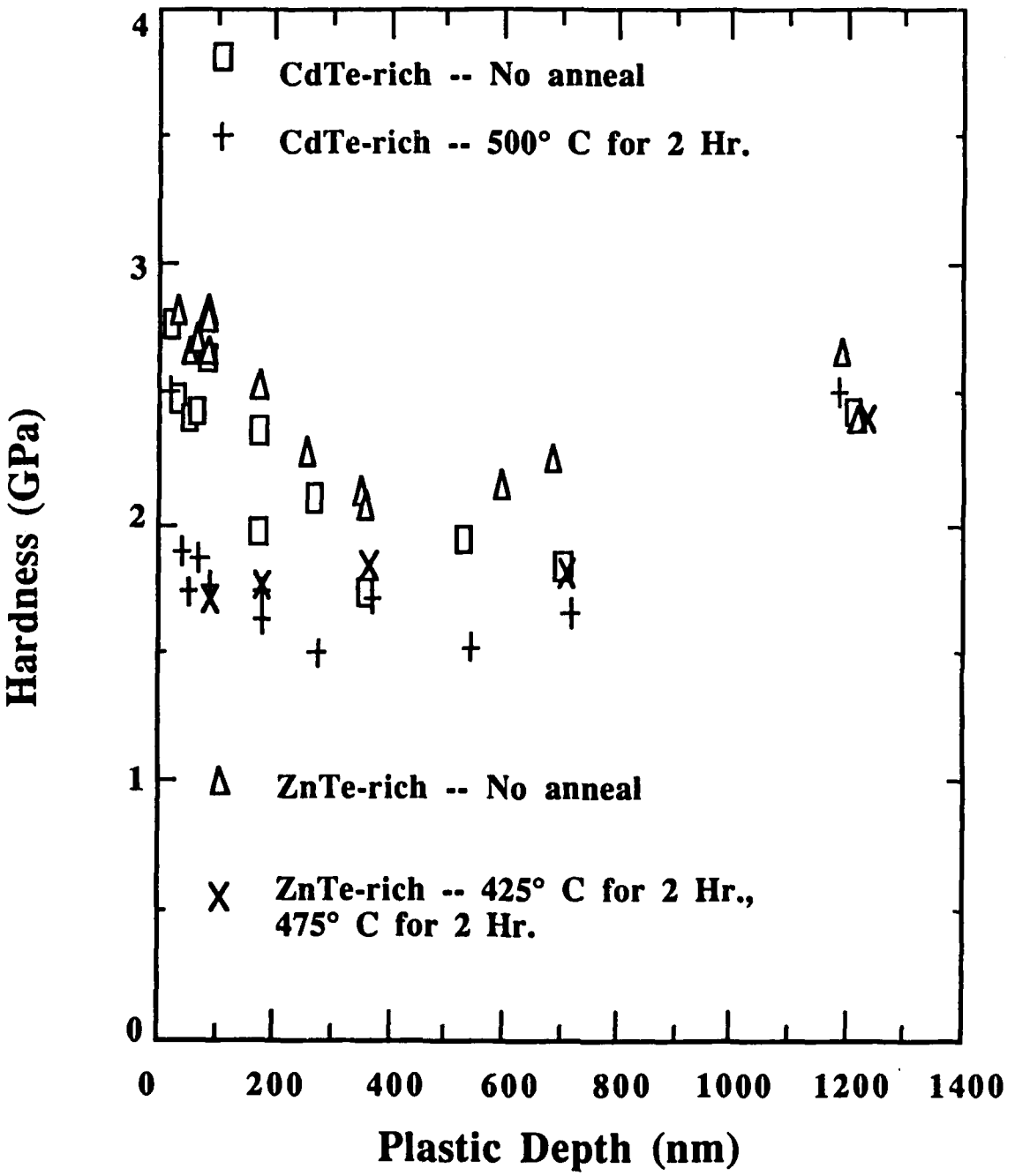

Figure 11. Hardness of ZnTe-CdTe superlattices as a function of plastic depth

Figure 12.

X-ray diffraction pattern of superlattice sample with 200 cycles of 25 Å ZnTe and 50 Å CdTe, 1.0 um ZnTe buffer layer, and (100) GaAs substrate -- No anneal

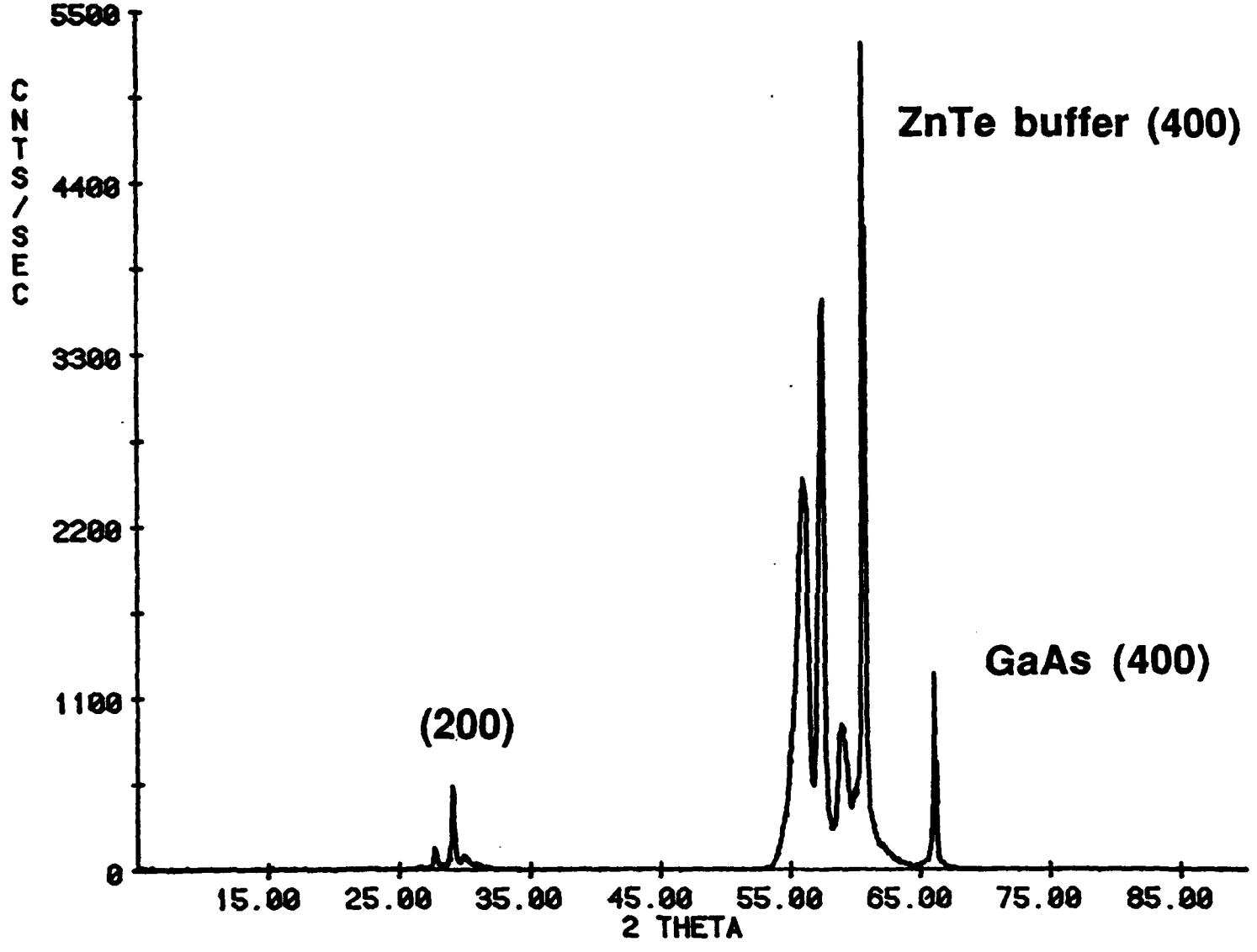

Figure 13. **X-ray diffraction pattern of superlattice sample with 200 cycles of 25 Å ZnTe and 50 Å CdTe, 1.0 um ZnTe buffer layer, and (100) GaAs substrate -- Anneal at 500° C for 2 hr.**

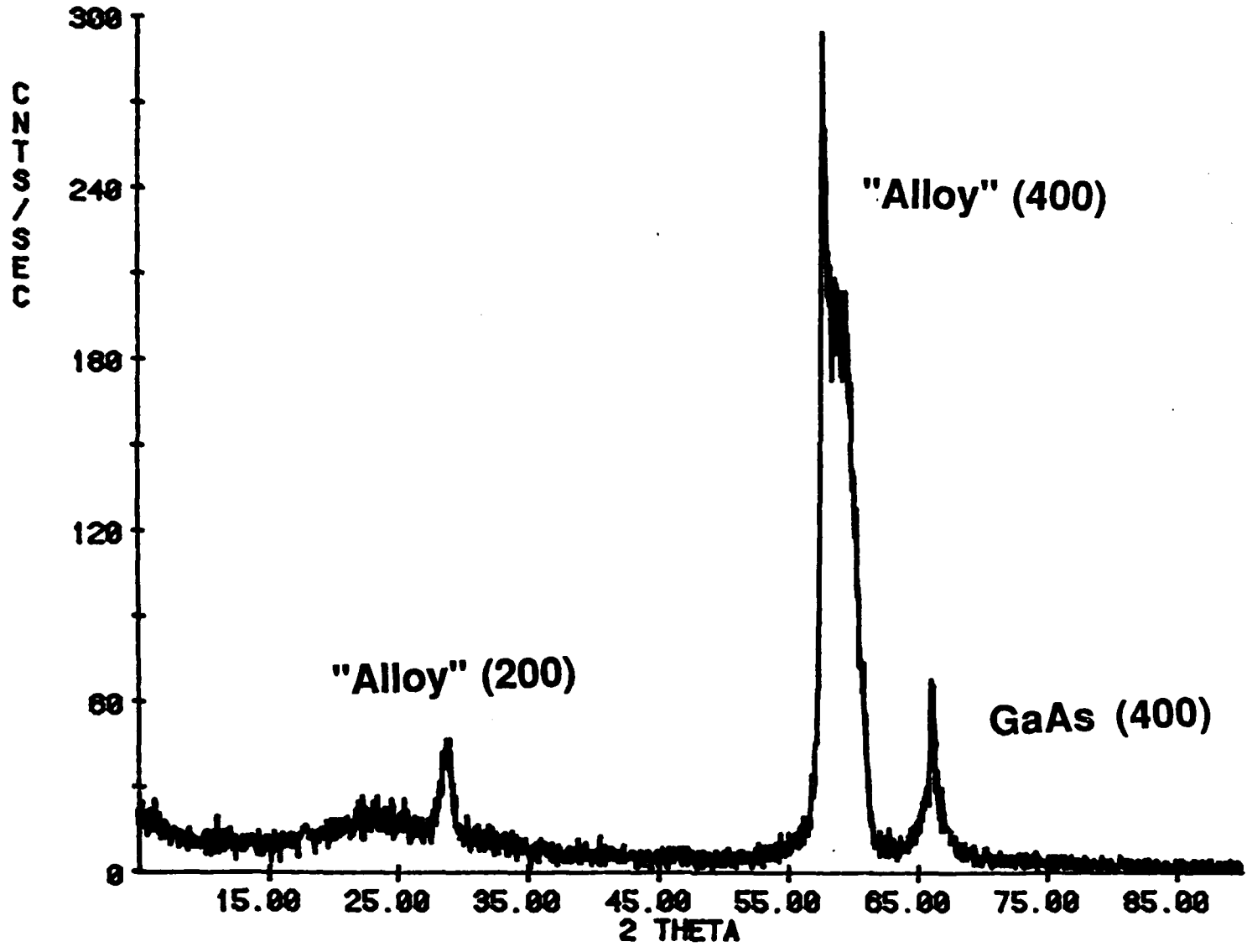

Figure 14. **X-ray diffraction pattern of superlattice sample with 200 cycles of 50 Å ZnTe and 25 Å CdTe, 1.0 um ZnTe buffer layer, and (100) GaAs substrate -- No anneal**

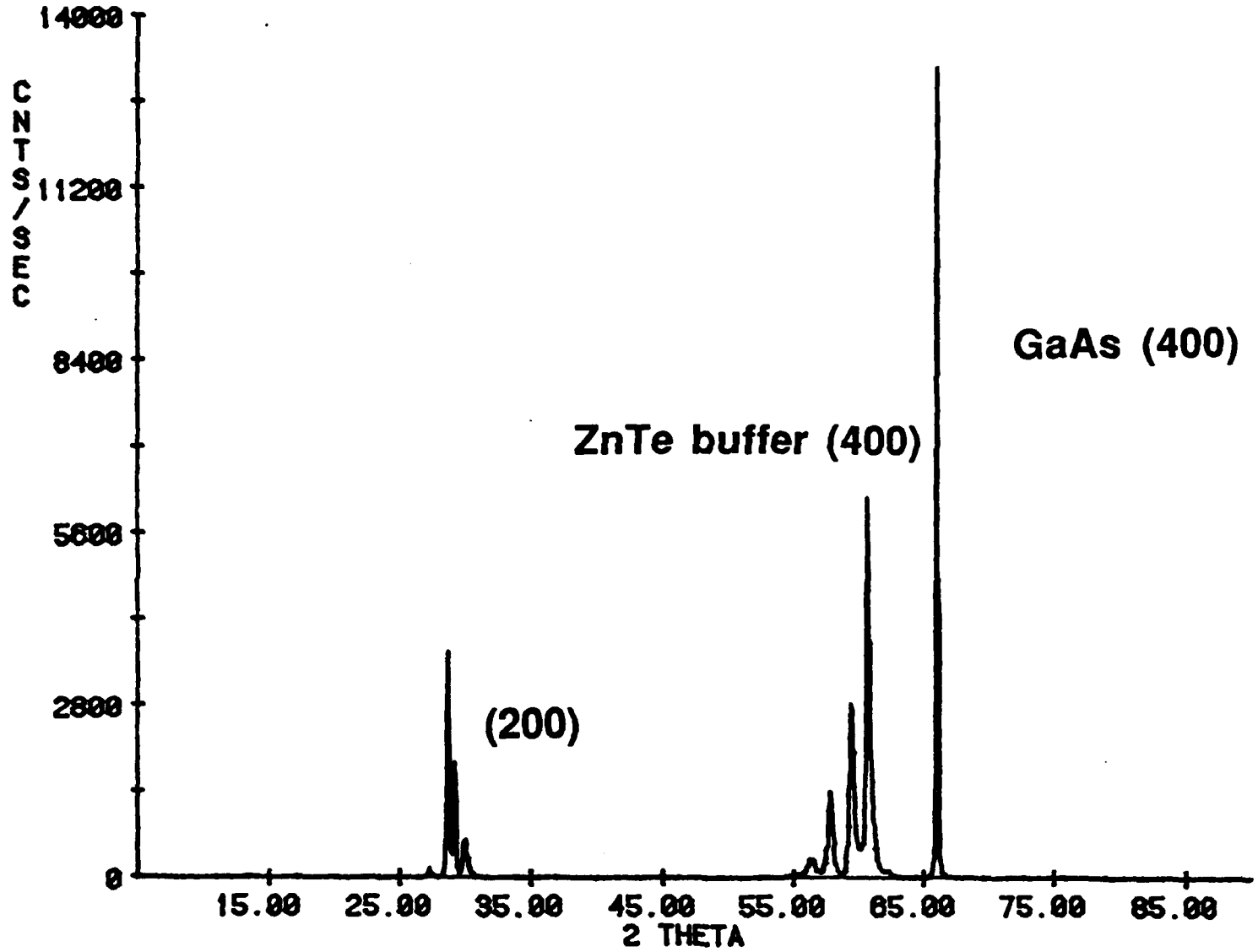

Figure 15. **X-ray diffraction pattern of superlattice sample with 200 cycles of 50 Å ZnTe and 25 Å CdTe, 1.0 um ZnTe buffer layer, and (100) GaAs substrate -- Anneal at 425° C for 2 hr. and at 475° C for 2 hr.**

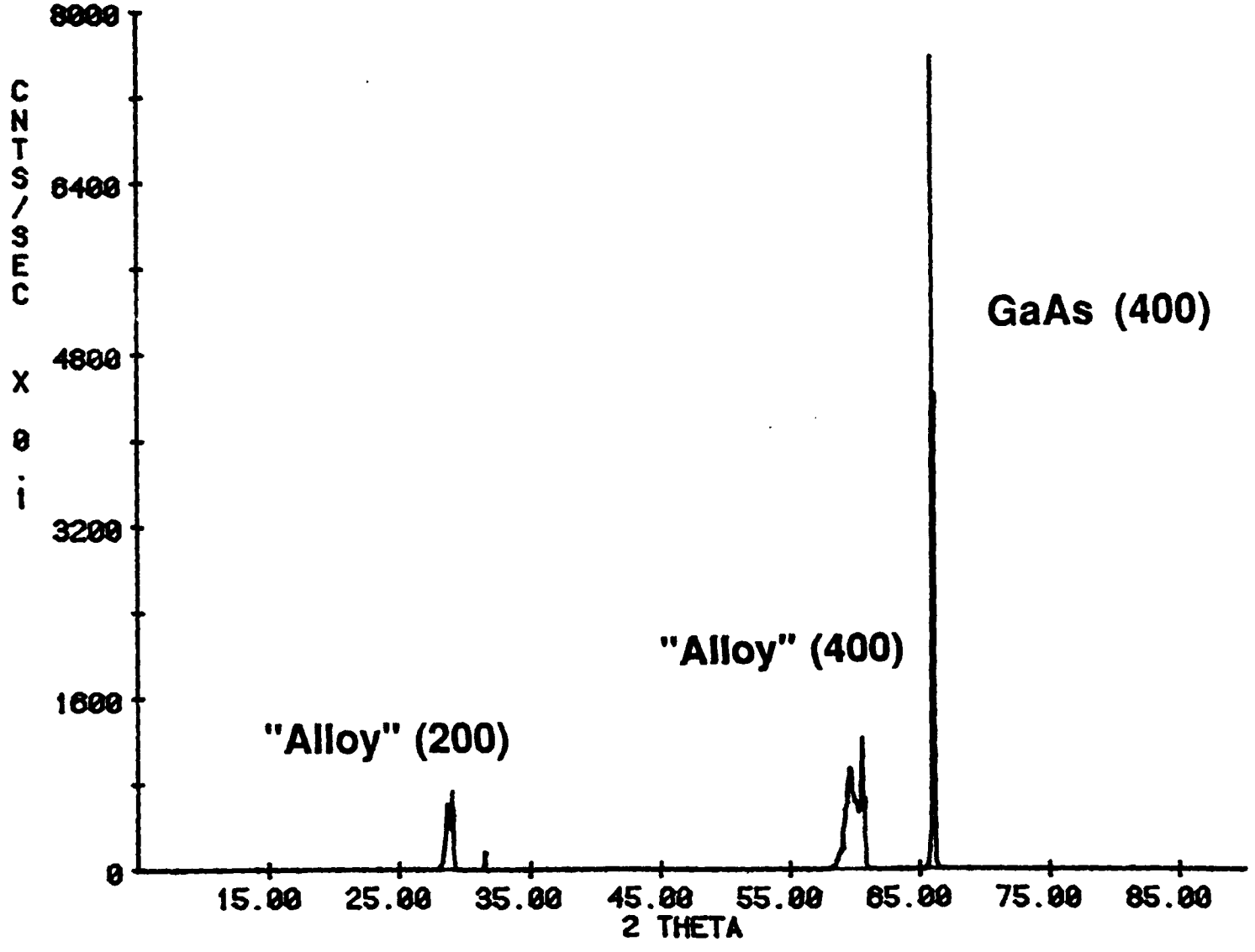

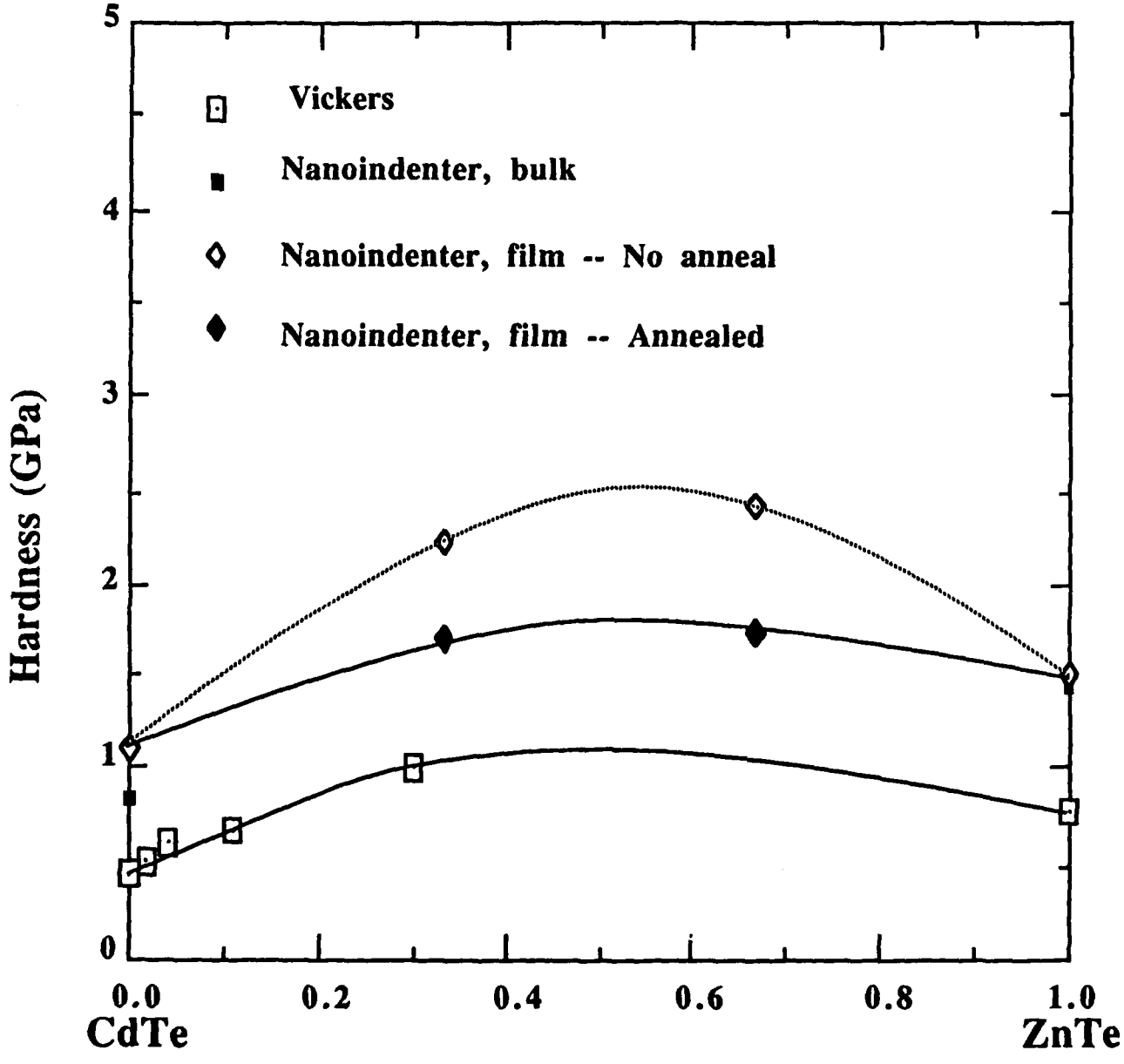

Figure 16. Hardness as a function of ZnTe fraction in epilayer and bulk ZnTe and CdTe and in ZnTe-CdTe superlattices

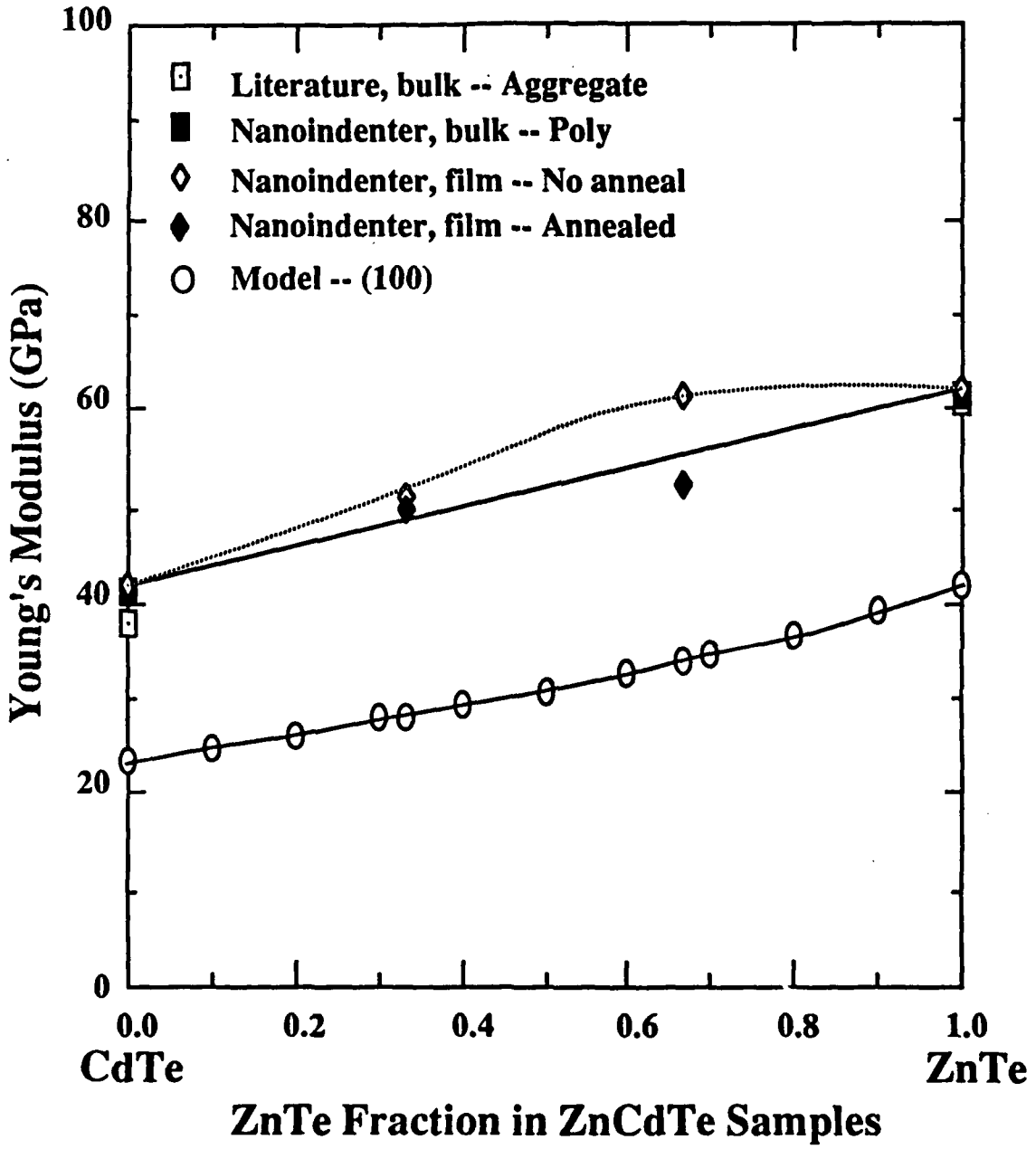

Figure 17. Young's moduli as a function of ZnTe fraction in epilayer and bulk ZnTe and CdTe and in ZnTe-CdTe superlattices

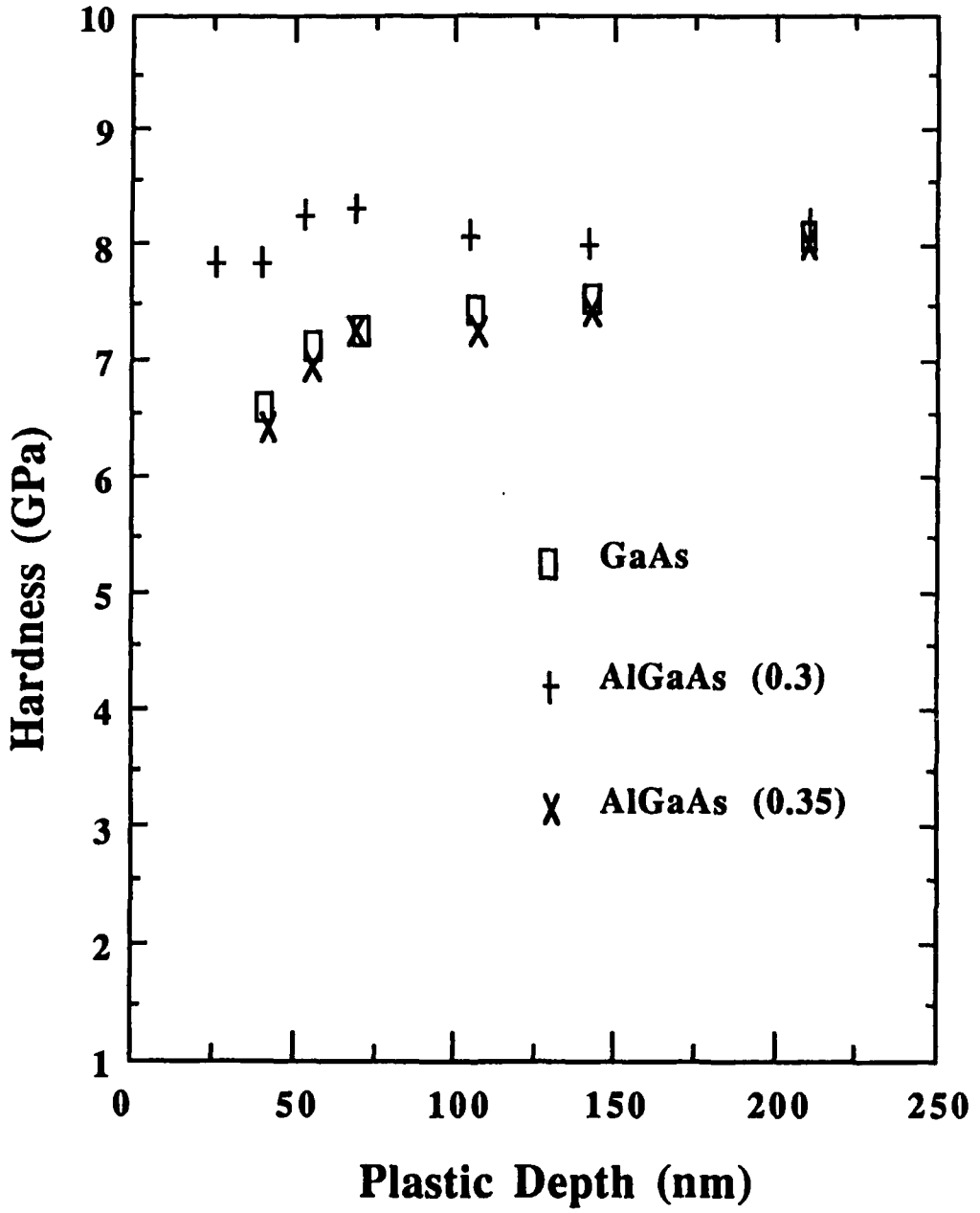

Figure 18. Hardness of a (100) GaAs substrate and two thin films of AlGaAs as a function of plastic depths

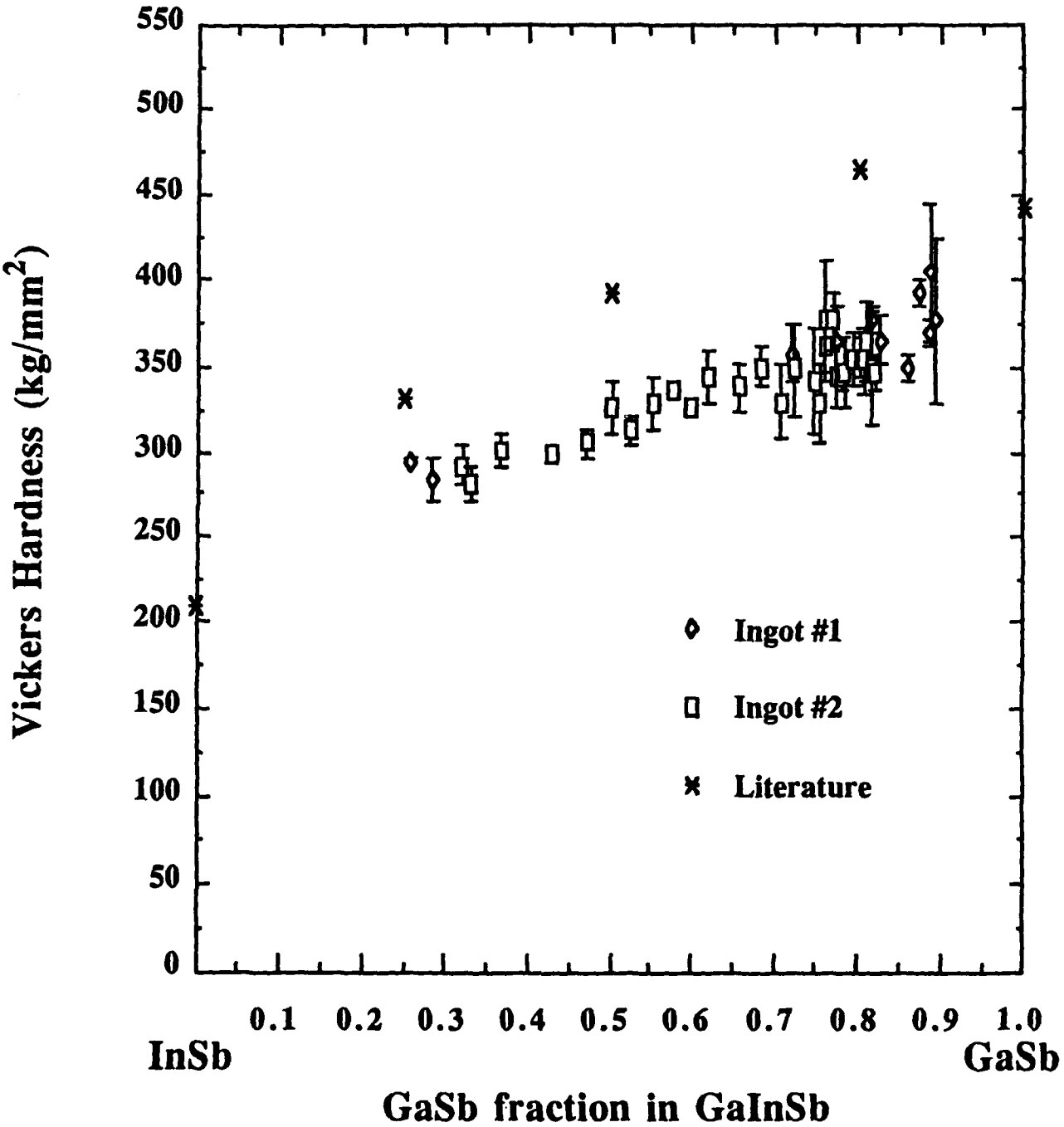

Figure 19. Vickers hardness as a function of GaSb fraction in GaInSb (our data and data from [24])

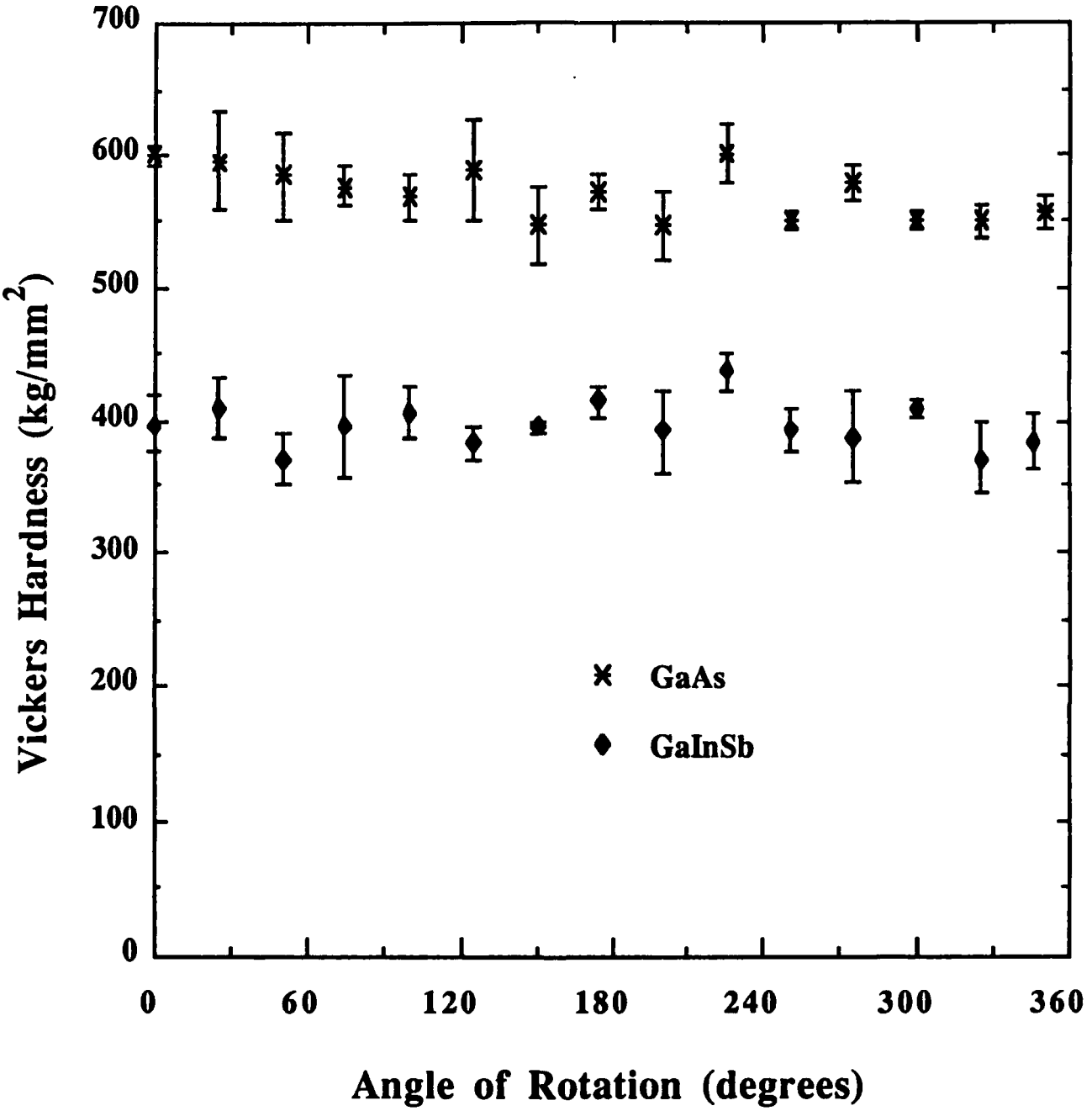

Figure 20. The effect of the angle of rotation on Vickers hardness on a (100) GaAs substrate and a (110) GaInSb ingot. Error bars are ± one standard deviation.

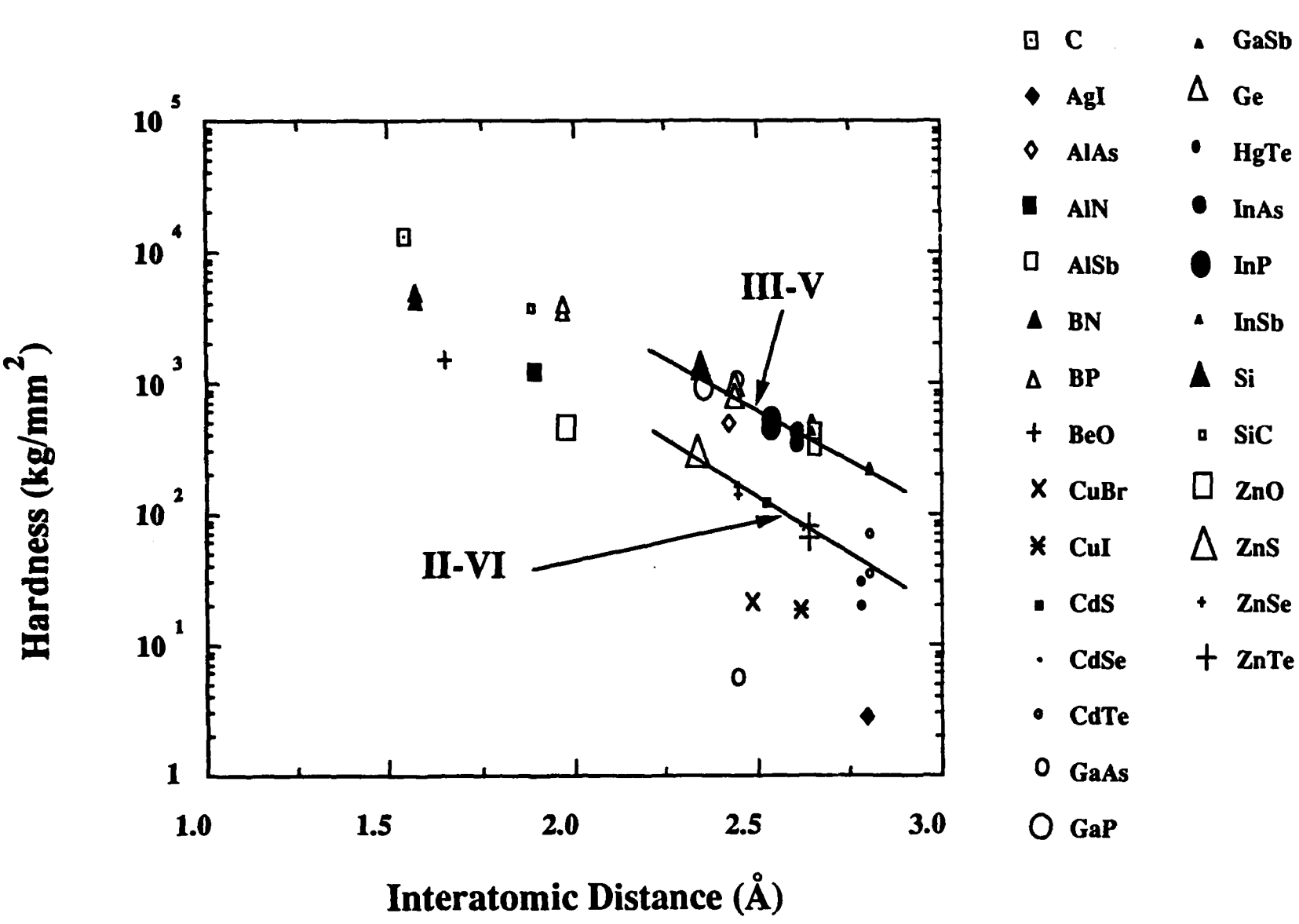

Figure 21. Hardness versus bond length (literature values)